

# Methods and Metadata for Ecological Effects of Sea Level Change Project

Lisa Marrack<sup>1</sup>, Laura Flessner, Rebecca Most, Chad Wiggins<sup>2</sup>, Zach Ferdana  
2017

<sup>1</sup> [lisamarrack@gmail.com](mailto:lisamarrack@gmail.com), affiliated with University of Hawaii, Hilo, HI

<sup>2</sup> [cwiggins@tnc.org](mailto:cwiggins@tnc.org), The Nature Conservancy of Hawaii, Kamuela, HI

Funded by NOAA-NCCOS.



## Table of Contents

Introduction.....	3
Flood Mapping Approach.....	3
Overview of Flood Mapping Methods.....	4
Goals.....	5
Caveats and Assumptions.....	5
GIS Layers.....	6
Details of Mapping Methods.....	7
Details of GIS Processing.....	9
Risk Factors.....	11
Conservation and Restoration Factors.....	12
Acknowledgements.....	13
References.....	14
Appendix 1: Rankings for relative risks and solutions.....	16
Appendix 2: Marra and Genz (2018): Sea Level Rise Analysis.....	18

## Figures

Figure 1. Study Area.....	7
Figure 2. Mean groundwater elevations above Local Mean Sea Level.....	8

## Tables

Table 1. Elevations above MHHW (meters) used to map frequency of flooding scenarios.....	5
--	---

## **Introduction**

This document describes the process used to map sea level rise inundation effects on anchialine pool ecosystems in West Hawai'i. The Nature Conservancy's (TNC) Coastal Resilience program supports practitioners around the world who are working to address coastal hazards with adaptation and risk mitigation solutions. In partnership with scientists from the National Oceanic and Atmospheric Administration (NOAA), the Conservancy led the development of the "Ecological Effects of Sea Level Change" application (app), a web-based decision support tool to help planners understand the potential future risk to anchialine pool ecosystems. Understanding the magnitude and urgency of risk will help prioritize pool conservation/restoration actions, inform regional coastal habitat management, and influence future development decisions.

Anchialine pools present an ideal focal ecosystem target for this risk assessment tool. Anchialine pools, also known locally as *loko wai 'opae*, are coastal water features that have no overland connection to the ocean, but are connected to the marine environment through the underground porous substrate. This subsurface connection enables fresh groundwater from upslope areas to mix with marine waters (Holthuis 1973). In Hawaii, the subterranean connection to the ocean is apparent as pool surface elevations rise and fall with the daily tidal cycle (Oki 1999, Marrack 2015). Because they exist at the interface between freshwater and seawater, anchialine pools represent an ideal system for understanding water quality and host a unique biology. The endemic shrimp *Halocaridina rubra* and *Metabetaus lohena* (opae'ula); endangered species such as the shrimp *Procaris hawaiiana* and the damselfly *Megalagrion xanthomelas*; and other rare species rely on these habitats (Maciolek and Brock 1974, US Fish and Wildlife Service 2017, Sakihara 2012). Introduced fishes, changes in land-use that contribute to habitat loss, reductions or impairments of freshwater water quantity and quality, overgrowth by introduced vegetation, and rising sea levels threaten the integrity of pool ecosystems (Capps et al. 2009, Carey et al. 2010, Brock and Kam 1997, Marrack et al. 2015, Marrack 2016).

Visualizing future scenarios enables more effective management decision-making for anchialine pool ecosystem conservation. Additionally, the data demonstrating anchialine pool impacts can inform impacts to other coastal ecosystems and features.

## **Flood Mapping Approach**

Maps were created to visualize potential impacts to anchialine pools due to coastal flooding that could potentially occur during 2030, 2040, 2050, and 2080 time periods. Flood predictions incorporated field surveys of over 500 anchialine pools, in-situ measurements of local groundwater levels (collected at 12 sites over a year), high resolution LiDAR-based topographic data, and probabilistic projections of future sea levels in the region (Marra and Getz 2018). The analysis of changes in flood frequency and magnitude at different time periods and its connection to changes in local groundwater levels enabled us to determine when current pools could be inundated by the ocean and where future pools could appear. In unconfined coastal aquifers such as in West Hawaii, the groundwater table is elevated above Mean Sea Level sloping up and away from the shoreline, and typically moves in response to changes in ocean level (Oki, 1999). As a result, groundwater may exacerbate inundation as sea levels rise (Bjerklie et al., 2012). Changes in ocean and groundwater levels will directly affect groundwater-fed anchialine pool habitats and the species within them (Marrack 2016).

Based on widespread field observations of daily tidal fluctuations in groundwater levels within wells and anchialine pools, it is assumed that there is high connectivity between ocean and groundwater across the study site (Oki 1999, Marrack 2015). Because anchialine pools require water to be present most days of the year, we were interested in flood frequency data as well as extreme water levels. We assume that a new pool will emerge on the landscape when a natural area begins to flood most days of the year. In pools that go dry everyday, endemic shrimp (opae'ula) and other pool species can be observed coming out of the subterranean aquifer up to the groundwater surface to graze on the substrate during higher tides.

Our approach differs from many sea level rise analyses that focus on extreme water levels and risk assessments for coastlines and coastal infrastructure. From the anchialine pool ecosystem perspective, more frequent flooding that might be considered “nuisance flooding” in an area with human infrastructure, is an opportunity for new pool habitats to form. However, extreme flooding might negatively impact pools due to dispersal of introduced fishes. We have worked to incorporate both aspects of sea level rise effects on pool habitats.

### **Overview of Flood Mapping Methods**

Regional sea level rise projections from Sweet et al. (2017) were combined with flood frequency and flood extreme analyses derived from observed water levels at local tide gauges to determine the plausible range in changes in the Still Water Level (SWL) at different time periods. Scenarios of water levels incorporate local tides and storm surge, regional patterns of atmospheric and oceanic circulation, and regional patterns of vertical land motion, as well as global changes in absolute sea level. Details of the analyses to derive SWL elevations for this project are described in Marra and Genz (2018). Summary tables of SWL scenarios are below (Table 1).

To make flood maps for a specific SWL projection, any coastal areas that were lower in elevation than the SWL of interest, were represented as inundated with water. Then, models of groundwater levels above sea level were used to determine flooding that would be associated with each SWL scenario in inland areas. To generate spatial data layers for the mapping application, flood maps combine the SWL “bathtub” mapping approach in areas adjacent to the ocean with additional inland flooding due to groundwater.

At each time period included in the app, flood maps were created to represent flood frequency according to four ranges: frequent, semi-frequent, infrequent and rare flooding. Frequent flooding is defined as flooding that occurs daily to every other day. Semi-frequent flooding will occur on a weekly to monthly basis. Infrequent flooding might happen one to several times a year. For each of these first three categories, the maps show a range of return intervals such that areas with a high likelihood of being inundated at a specific flood frequency are indicated in one color and areas with a lower likelihood of inundation at that frequency are indicated in another color (Marra and Genz 2018, Table A-1). Rare flooding represents areas that are expected to flood once in multiple decades. These rare flooding elevations were derived from the extreme SWL analysis rather than the flood frequency analysis (Marra and Genz 2018).

## **Goals of Mapping**

- Use the most update ocean water level predictions for the region.
- Improve precision by incorporating field measured elevation and groundwater levels into flooding maps because groundwater is higher than Mean Sea Level in the study area.
- Map sea level rise on top of Mean Higher High Water (MHHW, 0.376m).
- Incorporate accurate maps of current and future anchialine pools with and without invasive fish.
- Analyze potential dispersal of introduced fishes due to connectivity at high water levels.
- Provide a screening tool to identify areas of concern and facilitate data sharing with managers and decision-makers.

## **Caveats and Assumptions**

- The data and web app are meant to be used as screening tools for planning, educational, and public awareness purposes only and should not be used for legal purposes, site level planning, or permitting.
- The mapping does not incorporate future changes in coastal geomorphology such as erosion.

**Table 1: Elevations above MHHW (meters) used to map frequency of flooding scenarios. Current time period is data from the local tide gauges at 2005. These values are from the frequency of flooding analysis displayed in Marra and Genz (2018) Table A-1.**

Scenario	Frequent		Semi-frequent		Infrequent		Rare
	Low	High	Low	High	Low	High	High
Current	-0.2	0	0	0.1	0.2	0.3	0.5
2030	0.1	0.2	0.4	0.5	0.5	0.6	0.8
2040	0.2	0.4	0.5	0.7	0.6	0.8	0.9
2050	0.3	0.6	0.5	0.8	0.6	0.9	1.5
2080	0.5	1.4	0.7	1.6	0.8	1.7	1.9

## **GIS layers**

Descriptions of the Geographical Information Systems (GIS) layers created from the Sea Level Rise analysis

*Still Water Level flooding layers:* Areas flooded at a Still Water Level scenario. Each layer is a visual representation of all DEM elevations below a designated sea level elevation. SWL scenarios have a distinct time period (Recent, 2030, 2040, 2050, 2080); flood frequency (frequent, semi-frequent, infrequent, and rare); and likelihood (high or low) (Table 1).

*Groundwater flooding layers:* Areas inundated due to groundwater. Data is based on groundwater levels collected in pools and wells between August 2015 and June 2017. Groundwater calculations and GIS layers are created to match with specific SWL scenarios therefore are specific to time period (Recent, 2030, 2040, 2050, 2080); flood frequency (frequent, semi-frequent, infrequent, and rare); and likelihood (high or low).

*Current Shoreline:* The line extracted from the Digital Elevation Model that represents the 0- meter elevation at Local Mean Sea Level Datum.

*Current Anchialine Pools:* Current anchialine pools were mapped with a Trimble GeoXT Global Positioning System between 2011 and 2014. Some pools on private properties were digitized from Quickbird 2006 satellite imagery. The presence or absence of introduced fishes (tilapia and/or poeciliids) were recorded at the time of the surveys or were confirmed by property owners or land managers. If the fish status of a pool is unknown it is indicated as unknown in the attribute table.

*Future pools:* These are inland water features created at SWL frequency scenarios that flood at a minimum of 182 days a year. Generally, water bodies that hold water at least every other day and are not attached overland to the ocean will likely become new anchialine pools or wetlands in the porous basalt landscape of West Hawai'i. In GIS, future pools are flood polygons that: (a) do not intersect with the predicted ocean surface of a SWL scenario; (b) do not fall within a 13 m (43 ft) shoreline buffer at a SWL scenario; (c) and do not intersect with any polygon for a water body (fishpond or wetland) that is connected overland to the ocean. Each pool was ranked in terms of risk including the likelihood they will contain invasive fish or will connect with the ocean during infrequent flooding events. Risks due to development and cesspools were also added.

## **Details of Mapping Process**

This process is based on and describes tools and inputs in ESRI's ArcGIS software. Specifically, this process is intended for ArcGIS 10.3.1 and requires the Spatial Analyst extension.

### **Inputs**

#### **1. Digital elevation model (DEM)**

Elevation data are based on the 2016 release of LiDAR data from US Army Corps of Engineers. DEMs were built in LaStools with 1 m grids using the lowest elevation recorded in each grid. For the LIDAR topographic data, Horizontal Positional Accuracy is compiled to meet 1 m at 95% confidence level and Vertical Positional Accuracy of 19.6 cm at a 95% confidence level (10 cm RMSE).

#### **2. Still Water Levels from frequency and extreme value analyses**

Details of analyses to determine these values are described in Marra and Genz (2018).

#### **3. Groundwater level measurements and analysis**

Groundwater elevations above sea level were measured within 12 anchialine pools, fishponds and wells along the West Hawaii Sentinel Site. Water level sensors (In-Situ Rugged Troll 100) collected data at 5 or 15 minute intervals for over a year at each location starting in August of 2015. At each level logger position, semi-permanent benchmarks were established using CHC X90-OPUS (GPS) receivers during September, 2015 and July, 2016 by NOAA, TNC and Ed Carlson of the Geodetic Survey. These surveyed control points allowed us to calculate the mean groundwater level over sea level as well as examine the effect of tides on groundwater heights with high vertical resolution (5 cm). Data showed that as expected, mean groundwater levels are elevated above mean sea level and that these heights increase with distance from shore (Figure 2). Furthermore, data support previous observations from Kaloko-Honokohau National Historical Park (Figure 2). Data were therefore pooled with the Kaloko-Honokohau water levels and a new function was determined using established methods (Marrack 2015).

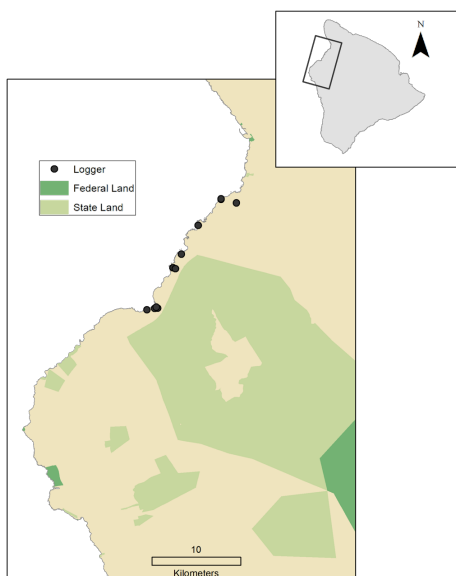


**Figure 1: Study area with groundwater logger locations. State and federal lands are shown.**

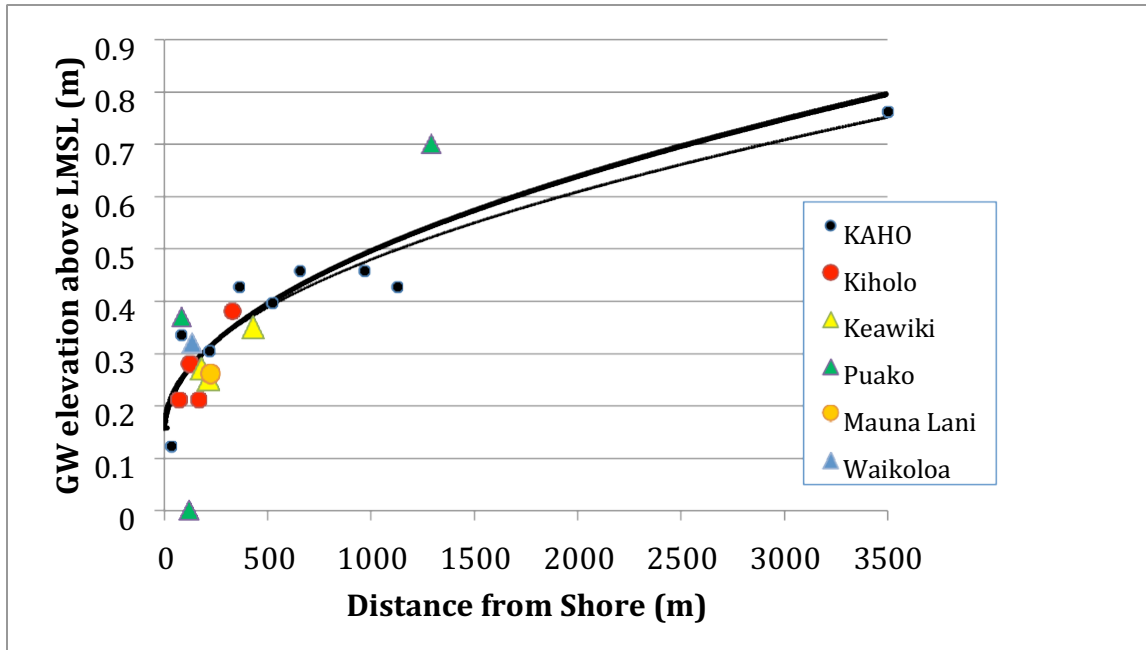


**Figure 2: Mean groundwater elevations above Local Mean Sea Level (LMSL) as a function of distance from shore (m). Data from 12 groundwater level logger sites are plotted along with 9 groundwater level sites monitored by the USGS from 2009-2010. The top curve represents the function calculated using all 21 data points ( $R_2 = .7995$ ). The bottom curve represents the function calculated by Marrack (2015) using the USGS data from 2009-2010. Note how closely the results from this study and 2015 are in agreement.**

Groundwater levels in an unconfined, homogenous aquifer, such as the aquifer in West Hawaii, are expected to be a function of the square root of distance from the shoreline (Glover 1959). Using our data for West Hawaii, the equation describing mean groundwater level as a function of distance from shore is:

$$H_{GW} = (0.010883 * (\sqrt{d}) + 0.15234) + SLR$$

**Where:**

$H_{GW}$  = Groundwater level above Mean Sea Level at any scenario (meters).

$d$  = distance from shore (meters).

SLR = the sea level rise change without the tidal component.

To account for the effect of tides on groundwater, a tidal efficiency component was also computed and multiplied to the MHHW (0.376 m). This part of the model accounts for the fact that tidal effects on groundwater decrease with increased distances from shore. The equation below is the tidal component of groundwater heights above Mean Sea Level (MSL).

$$H_{\text{tef}} = ((\text{Exp}(-0.2779 + (-0.0003321 * d))) * 0.376)$$

**Where:**

$H_{\text{tef}}$  = Tidal component of groundwater level above MSL

$d$  = distance from shore (meters)

Based on this model, the total groundwater height ( $H_{\text{total}}$ ) at a distance from shore at MHHW (0.376m) would be equal to the combined height of the Groundwater above sea level and the tidal component.

$$H_{\text{total}} = H_{\text{GW}} + H_{\text{tef}}$$

**4. Pool survey data.**

Pool surveys were primarily conducted in 2011-2014 (Marrack et al. 2015). Additional observations were included throughout the course of this study in 2016 to 2018.

**GIS Processing**

1. Because DEM vertical data is relative to Local Mean Sea Level (LMSL), the Still Water Levels to be used for Sea Level Rise scenarios were adjusted so that they were relative to LMSL.  $\text{SWL} + 0.376\text{m}$ .
2. Still Water Level (SWL) flood scenarios extracted from DEM.
  - a. In Spatial Analyst, using Raster Calculator tool: extract where the DEM height is less than the Still Water Level (SWL)
  - b. Convert Raster to Polygon features.
  - c. Delete any polygons that = 0 (not lower than SWL).
3. Groundwater flood layers (a unique groundwater layer was made to be paired with each SWL flood scenario)
  - a. For each SWL flood layer, the large polygon that covers the ocean up to the shore is selected and saved as the “ocean” layer for that sea level scenario.
  - b. In preparation for making Euclidian distance rasters that only stretch inland, create a Mask polygon that covers the shoreline of the study area and stretches over 1 km inland.
  - c. A Euclidian distance raster (2 m grid) is created with respect to the SWL “ocean” layer. Use the Mask polygon to constrain the distance raster reaching inland. This creates a raster starting at the unique “shoreline” of each sea level scenario.
  - d. For groundwater rasters, a groundwater level is calculated within each 2 m grid of the

Euclidean distance raster using the groundwater level and tidal efficiency functions calculated from the groundwater level logger data. The “SWL value” is the specific sea level rise level being examined. In the spatial analyst toolset, select Raster Calculator tool, and input:

“((Exp(-0.2779 + (-0.0003321 \* "EuclidianDistanceRaster")) \* 0.376)  
+ (0.010883\*(SquareRoot("EuclidianDistance Raster")) + 0.15234) + (SWL value)”

- e. To extract areas that will be flooded due to groundwater, we used the Spatial analyst toolset, and the Raster Math tool. Extract locations where the DEM value is less than the Groundwater Raster value.
  - f. Convert groundwater flooded area Raster to Polygon feature.
  - g. Delete all polygons that are = 0 (not flooded).
4. Create future anchialine pool polygon features for 2030, 2040, 2050 and 2080. These pools are determined to be those that are flooded at least 185 days a year (or every other day). Using the SWL flooding frequency data (Table 1) we assigned the following flood levels as those that would likely be the threshold at which flooded areas will become flooded frequently enough to become new pool habitats.

$$2030 = 0.2 + \text{MHHW}$$

$$2040 = 0.2 + \text{MHHW}$$

$$2050 = 0.4 + \text{MHHW}$$

$$2080 = 0.9 + \text{MHHW}$$

- a. Using the groundwater layer for that scenario, select flooded areas that:
  - Are not intersecting, connected, or within 13 m of the ocean.
  - Are not intersecting, connected, or within 2 m of fishponds connected overland to ocean.
  - Are not in paved or similarly developed land use type as defined by visual inspection of aerial imagery and C-CAP layers (NOAA 2011).

These selected inland areas are saved as the pools for the specified time period.

- b. Define pool status in attribute tables (summarized in Appendix1).

## RISK FACTORS

- Under the attribute column “EXISTING”, pools that are currently existing are assigned a 1 and if they are new they are assigned a 0. The pools that currently exist will not be shown when users zoom into the online App to protect locations.
- Under the attribute column “INVASIVE”, existing pools with introduced fish are assigned a 40 and if not they are a 0. For 2030, 2040, 2050 and 2080 pools, pools are assigned a 40 if an existing pool with fish becomes connected overland to another pool due to a flood polygon from the yearly high flood level. We assume that this overland connection provides a risk potential for introduced fishes to disperse. Pools where the existence of invasive species has not been determined are assigned 255.
- Under the attribute column “OCEAN”, pools that are connected overland to the ocean with the semi-frequent (weekly to monthly) flooding frequency layers (or within 15 m of connection with the ocean) are assigned a 40. Those pools that are connected overland to the ocean with the infrequent (annual) flood frequency layers (or within 15 m of the connection with the ocean) are assigned a 20. Infrequent connection to the ocean is not a large issue for pools but frequent connection indicates they will soon become part of the marine environment.
- Under the attribute column “FUT\_DEV”, future pools that intersect proposed future development may be at risk. However, these areas may be targets to try to influence future development. Using the County of Hawaii’s Land Use Pattern Allocation Guide, pools that intersect with planned conservation or open areas are assigned 0 (low risk), pools that intersect with areas proposed for low density development are assigned 20 (medium risk), and pools that intersect with areas proposed for med-high density development, urban expansion, or industrial are assigned 40 (high risk).
- Under the attribute column “CESS”, using the On-Site Sewage Disposal Systems (OSDS) Risk Severity Score (Whittier et al. 2014), if an anchialine pool is within a buffered distance (determined by OSDS risk factor  $\wedge 2$ ) of a cesspool at risk, that anchialine pool could have a higher likelihood of contamination. Pools located near a "Low" risk cesspool (0-5 OSDS score) are assigned 0, pools located near a "Medium" risk cesspool (6-15 OSDS score) are assigned 20, and pools located near a “High” risk cesspool (>15 OSDS score) are assigned 40.
- The attribute CUMULATIVE RISK, aggregates all of the risk factors described

above. The CUMULATIVE RISK index is calculated by adding all of the other risk scores together.

## CONSERVATION & RESTORATION FACTORS

- Pools that contain invasive species can be targeted for removal to restore the natural ecosystem functions of the pool. Under the attribute column “RESTORE”, pools that are at low risk of invasive species transmission are assigned 0, pools that are at a medium risk of invasive species are assigned 40, pools that have yet to be surveyed to determine if invasive species already exist are ranked 255.
- Pools that are not on legally protected land and may be impacted by future development are at higher risk and a priority for future conservation. Under the attribute column “PROTECT”, pools that are already on legally protected land and have a low risk of being impacted by future development are assigned 0 (lower conservation priority), pools that are NOT on protected land AND have a medium or low risk of being impacted by future development are assigned 20 (medium priority), and pools that are NOT on protected land AND have a high risk of being impacted by future development are assigned 40 (high conservation priority).

## **Acknowledgements**

**Funding:** NOAA/ National Center for Coastal Ocean Science (David Kidwell, manager).

**Project Team:** John Marra, Doug Harper, Ed Carlson (NOAA); Ayesha Genz (University of Hawai‘i); Lisa Marrack (UC Berkeley and University of Hawai‘i); Chad Wiggins, Laura Flessner, Zach Ferdana, Kim Falinski, Rebecca Most, Julia Rose, Cecile Walsh, Bert Weeks, Eric Conklin (TNC); Ku‘ulei Keakealani – voice on app (Hui Aloha Kīholo)

**App Development Workshop Participants:** Bethany Morrison, Kevin Sullivan (Hawai‘i County Planning Department); Scott Laursen, Tracy Wiegner, Ryan Perroy, Rose Hart (University of Hawai‘i at Hilo); Rick Gmirkin, Aric Arakaki (Ala Kahakai National Historic Trail, NPS); Amanda McCutcheon, Kailea Carlson (NPS); Lisa Ferentinos (UH SeaGrant); Maya Walton (UH Seagrant/NOAA); Brad Romine (Seagrant/DLNR-OCCL); Matt Wung (USDA/Natural Resource Conservation Service); Hannah Connelly (NRCS/Mauna Kea Soil and Water Conservation District); Dena Sedar (Hawaii State Parks); Ryan Priest (Mauna Lani); Keoki Downes, Reggie Lee (Kohanaiki); Kauhane Morton, Will Suliban (Kūki‘o); Ku‘ulei Keakealani, Lehua Kamaka, (Hui Aloha Kīholo); George Fry, Robby Robertson (Puakō Community Association); Erica Perez (Coral Reef Alliance); Lindsey Kramer (Division of Aquatic Resources).

Previous work by Lisa Marrack examining the effects of introduced fishes and sea level rise on anchialine pool ecosystems in Hawaii was supported by the Californian Cooperative Ecosystem Studies Unit Project of the National Park Service and the University of California Regents at Berkeley (Task Agreement J8C07100018). This previous work provides some of the basis for the Ecosystem Effects of Sea Level Rise Project described here.

## **References**

- Brock, R.E., and A.K.H. Kam. 1997. Biological and water quality characteristics of anchialine resources in Kaloko-Honokohau National Historical Park. Cooperative national park resources studies unit, technical report 112. Honolulu: University of Hawai‘i at Manoa.
- Capps, K. A., C. B. Turner, M. T. Booth, D. L. Lombardozzi, S. H. McArt, D. Chai, and N. G. Hairston Jr. 2009. Behavioral responses of the endemic shrimp *Halocaridina rubra* (Malacostraca: Atyidae) to an introduced fish, *Gambusia affinis* (Actinopterygii: Poeciliidae) and implications of the trophic structure of Hawaiian anchialine ponds. *Pacific Science*, 63: 27-37
- Carey, C. C., M. P. Ching, S. M. Collins, A. M. Early, W. W. Fetzer, D. Chai, and N. G. Hairston Jr. 2010. Predator-dependent diel migration by *Halocaridina rubra* shrimp (Malacostraca: Atyidae) in Hawaiian anchialine pools. *Aquatic Ecology*. DOI: 10.1007/s10452-010-9321-0
- County of Hawaii. October, 2015. County of Hawaii’s Land Use Pattern Allocation Guide. Metadata at: <http://files.hawaii.gov/dbedt/op/gis/data/hawctylupag.pdf>
- Englund, R.E. 1999. The impacts of introduced poeciliid fish and Odonata on the endemic Megalagrion (Odonata) damselflies of Oahu Island, Hawaii. *Journal of Insect Conservation*, 3.3: 225-243.
- Glover, R.E. 1959. The pattern of fresh-water flow in a coastal aquifer. *Journal of Geophysical Research*, 64(4): 457–459.
- Holthuis, L. B. 1973. Caridean shrimps in land-locked saltwater pools at four Indo-West Pacific localities (Sinai Peninsula, Funafuti Atoll, Maui and Hawai‘i Islands), with a description of one new genus and four new species. *Zool. Verhand.* 128: 48 p.
- Maciolek, J. A. and R.E. Brock. 1974. Aquatic survey of the Kona Coast ponds, Hawai‘i Island. Sea Grant Advisory Report UNIHI-SEAGRANT-AR-74-04. University of Hawai‘i, Honolulu. 73 p.
- Marra, J. and A. Genz. 2018. Scenario-based Analysis of the Potential Impacts of Sea Level Rise on Coastal Flooding and Shoreline Retreat along the Kohala and Kona Coasts, from Kawaihae to Kailua-Kona, on the Island of Hawai‘i. NOAA Technical Report. 28 pgs.
- Marrack, L. 2015. Incorporating groundwater levels into sea-level detection models for Hawaiian anchialine pool ecosystems. *Journal of Coastal Research*, 31(5): 1170 – 1182.
- Marrack, L. 2016. Modeling potential shifts in Hawaiian anchialine pool habitat and introduced fish distribution due to sea level rise. *Estuaries and Coasts*, 39: 781. doi:10.1007/s12237-015-0025-5
- Marrack, L., S. Beavers & P. O’Grady, 2015. The relative importance of introduced fishes, habitat characteristics, and land use for endemic shrimp occurrence in brackish anchialine pool ecosystems. *Hydrobiologia*, 758: 107–122.

[NOAA] National Oceanic and Atmospheric Administration, Ocean Service, Coastal Services Center. 2011. C-CAP Land Cover, Hawai'i, 2005. [www.csc.noaa.gov](http://www.csc.noaa.gov).

Oki, D. 1999. Geohydrology and numerical simulation of the ground-water flow system of Kona, Island of Hawai'i. U.S. Geological Survey, Water-Resources Investigation Report 99-4073, Reston, Virginia.

Sakihara, Troy. 2012. A diel comparison of the unique faunal assemblage in remote anchialine pools on Hawai'i Island. *Pacific Science*, 66(1):83-95

Sweet, W.V., R.E. Kopp, C.P. Weaver, J. Obeysekera, R.M. Horton, E.R. Thieler, and C. Zervas (2017). Global and Regional Sea Level Rise Scenarios for the United States. NOAA Tech. Rep. NOS CO-OPS 083, 75 pp.

US Fish and Wildlife Service, <https://ecos.fws.gov>, accessed 2017

Whittier R. and A. El-Kadi. 2014. On-site Sewage Disposal Systems (OSDS) risk severity score distribution of Hawaii Island. Prepared for the State of Hawaii Department of Health. 257 pgs.

## Appendix 1: Rankings for Relative Risks and Solutions

Variable	Ranking	Rationale	Source
Pool	<b>Viable</b> = wet at least once every two days  <b>Not Viable</b> = all others	If flood frequency indicates the elevation where a new pool develops is wet at least once every 2 days, it is considered a viable pool.	Created from flood frequency elevations.
New pools cannot intersect existing impervious surface	<b>Viable</b> = does not intersect existing impervious surfaces  <b>Not Viable</b> = all others	New pools that intersect existing impervious areas, such as roads or parking lots, are not viable and have no potential for restoration/conservation.	Created from intersection of land cover data and flood frequency Elevations
<b>Risk Factors</b>			
Likelihood of ocean inundation	<b>Low</b> = no chance of connection to ocean in a year. (No overlap with annual flood layer - lower likelihood/ also not within 15 m of this layer)  <b>Med</b> = some chance of connection to ocean in a year (Overlaps with the annual flood layer [lower likelihood] and/or is within 15 m of this layer)  <b>High</b> = high chance of connection to the ocean in a year (Overlaps with the weekly/monthly flood layer [lower likelihood] and/or is within 15 m of this layer)	If a pool becomes connected to the ocean it may get too salty to sustain freshwater life.	Created from flood frequency elevations.
Intersects with area zoned for future development	<b>Low</b> = intersects with planned conservation or open areas  <b>Med</b> = intersects with areas zoned for low density urban or resorts  <b>High</b> = intersects with areas zoned for med-high density development, urban expansion, or industrial	If new pools intersect proposed future development, any restoration may be at risk. However, these areas may be targets to try to influence future development.	County of Hawaii <a href="#">Land Use Pattern Allocation Guide</a>
Likelihood of invasive species transmission	<b>Low</b> = likely not "connected" to another pool with fish any time in a year  <b>High</b> = "Connected" to another pool with fish at least 1 time/year	If "connected" to a pool with introduced fish at any time, there may be a high likelihood of invasive species transmission.	Created from flood frequency elevations and known fish locations.
Likelihood of cesspool contamination	<b>Low</b> = pool is located near a "Low" risk cesspool (0-5 OSDS score)  <b>Medium</b> = pool is located near a "Medium" risk cesspool (6-15 OSDS score)  <b>High</b> = pool is located near a "High" risk cesspool (>15 OSDS score)	If an anchialine pool is within a buffered distance (determined by OSDS risk factor ^2) of a cesspool at risk, that anchialine pool has a higher likelihood of contamination	<a href="#">2014 On-site Sewage Disposal Systems (OSDS) risk severity score distribution of Hawaii Island. Whittier et al.</a>

Conservation and Restoration Factors			
Suitability for restoration through invasive species removal	<p><b>Low</b> = pools that are at low risk of invasive spp transmission</p> <p><b>High</b> = pools that are at high risk of invasive spp transmission</p> <p><b>Unknown</b> = pool has yet to be surveyed to determine if it currently contains invasive species</p>	Pools that contain invasive species can be targeted for removal to restore the natural ecosystem functions of the pool.	Created from flood frequency elevations.
Suitability for conservation through land protection	<p><b>Low</b> = pools that are already on legally protected land and have a low risk of being impacted by future development</p> <p><b>Med</b> = Pools that are NOT on protected land AND have a medium or low risk of being impacted by future development</p> <p><b>High</b> = Pools that are NOT on protected land AND have a high risk of being impacted by future development</p>	Pools that are not on legally protected land and may be impacted by future development are at higher risk and a priority for future conservation	Legally protected lands and reserves. <a href="#">Hawaii State GIS</a> and County of Hawaii <a href="#">Land Use Pattern Allocation Guide</a>

## **Appendix 2: Sea Level Rise Analysis**

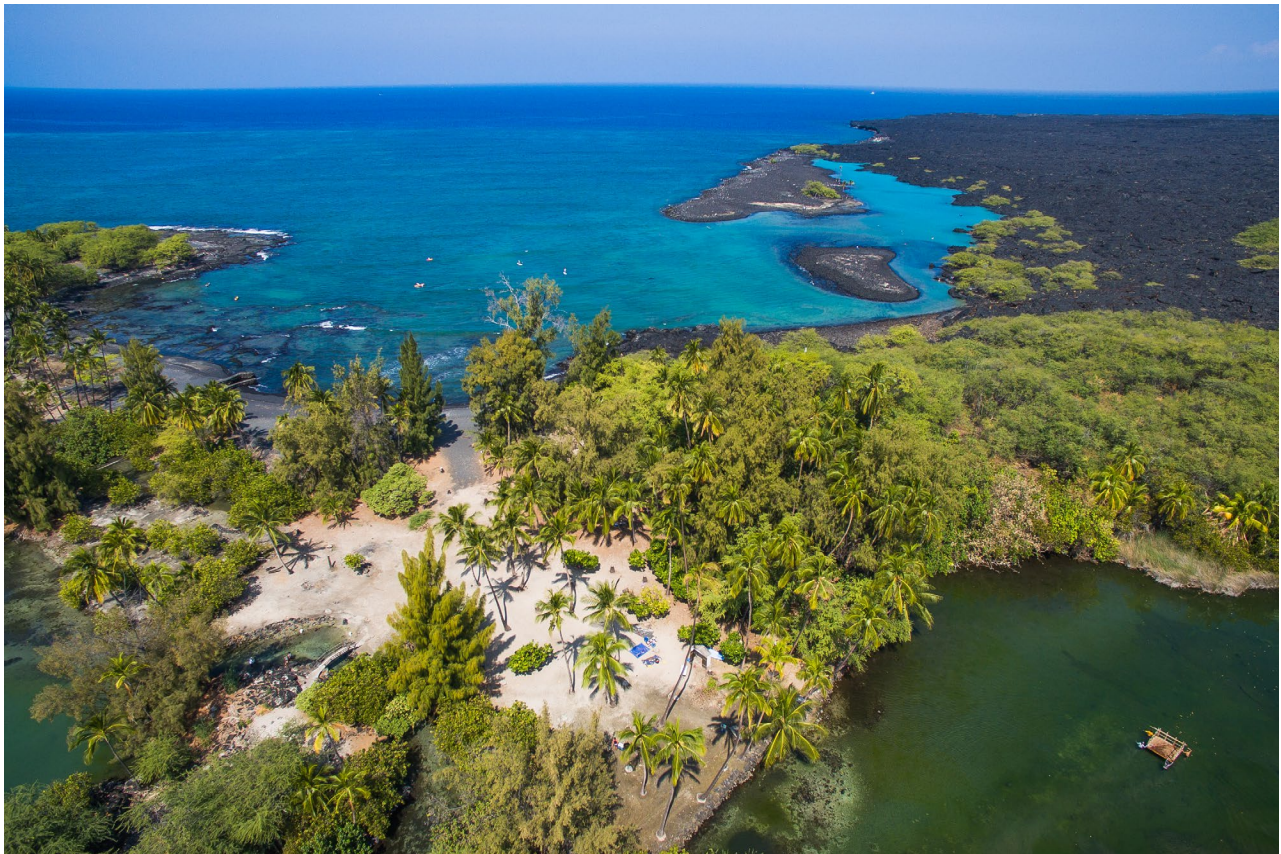
Marra, J. and A. Genz. 2018. Scenario-based Analysis of the Potential Impacts of Sea Level Rise on Coastal Flooding and Shoreline Retreat along the Kohala and Kona Coasts, from Kawaihae to Kailua-Kona, on the Island of Hawai'i. NOAA Technical Report. 28 pg

# Scenario-based Analysis of the Potential Impacts of Sea Level Rise on Coastal Flooding and Shoreline Retreat along the Kohala and Kona Coasts, from Kawaihae to Kailua-Kona, on the Island of Hawai‘i

## METHODS AND RESULTS

*John J. Marra<sup>1</sup> and Ayesha Genz*

*Updated January 17, 2018*



**Kiholo Fishpond.** *Photo Courtesy of Chad Wiggins, TNC.*

<sup>1</sup>NOAA NESDIS National Centers for Environmental Information (NCEI)

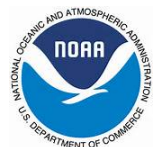


# Table of Contents

Figures.....	iii
Tables.....	iii
Overview.....	1
Background.....	2
Study Area and Data Sources.....	3
Methodology.....	4
Analysis of Flooding Extremes.....	5
Stationary EVA.....	5
Regional Frequency Analysis.....	7
Non-Stationary EVA.....	8
SWL Scenarios.....	9
Dynamic Still Water Levels.....	9
Wave Runup and TWL.....	10
Shoreline Retreat.....	13
Analysis of Flood Frequency.....	13
Results.....	15
SWL Scenarios.....	15
DWL Scenarios.....	16
TWL Scenarios.....	17
Shoreline Retreat Scenarios.....	17
Flood Frequency.....	18
Discussion.....	20
Conclusions.....	21
References.....	23
Appendix: Additional Information pertaining to the TNC EESLR Web Tool.....	26

## Figures

Figure 1. Total Water Level (TWL) Spectrum .....	2
Figure 2. Study Area.....	4
Figure 3. Beach Profiles at a) Kiholo and b) ‘Aimakapā. ....	5
Figure 4. Generalized Extreme Value (GEV) probability distribution function.....	7
Figure 5. Decomposition of extreme SWL at Kawaihae tide station. ....	8
Figure 6. Schematic of TWL.....	10
Figure 7. A combined time series from buoy #51001 and #51101 was used to assess runup.....	12
Figure 8. Probability of exceedance for annual records of hourly water levels at Kawaihae tide gauge...	14
Figure 9. Nuisance floods exceeding MHHW+0.1m at Kawaihae tide gauge.....	14

## Tables

Table 1. Tide Gauge stations used in SWL analysis.....	7
Table 2. SWL Scenarios. ....	15
Table 3. DWL Scenarios.....	16
Table 4. TWL Scenarios at Kiholo. ....	17
Table 5. Shoreline Retreat Scenarios at Kiholo.....	18
Table 6. Flood Frequency.....	19
Table A-1. Flood frequency used in the TNC EESLR Web Tool.....	27

*This document is an update of an earlier report (Marra and Genz, 2017) with a focus on Kiholo. Support for this work included funds provided to The Nature Conservancy through the NOAA Sentinel Sites Program and to the University of Hawaii Joint Institute of Marine and Atmospheric Research through the NOAA Coastal Storms Program.*

# Scenario-based Analysis of the Potential Impacts of Sea Level Rise on Coastal Flooding and Shoreline Retreat along the Kohala and Kona Coasts, from Kawaihae to Kailua-Kona, on the Island of Hawai'i

## METHODS AND RESULTS UPDATED

### Overview

Global mean sea level (GMSL) is projected to increase from one-third to more than two meters by the end of this century (Sweet et al., 2017). A series of analyses were conducted to evaluate how coastal flood magnitude and frequency might change along a section of shoreline extending from Kawaihae to Kailua-Kona, on the Island of Hawai'i in response to such sea level change. Analyses of flood frequencies derived from a normal distribution and flood extremes derived from a Generalized Extreme Value (GEV) distribution of observed water levels in tide gauges were combined with probabilistic projections of future regional sea levels to determine the plausible range in changes in the Still Water Level (SWL) at different time periods. Possible contributions to SWL attributable to climate variability, changes in sea level associated with changing patterns in atmospheric and oceanic circulation occurring on time scales of years to decades, were also accounted for. The results of these bounding analyses are expressed in a risk-based construct, where representative values are selected to represent the low, middle, and high end among calculated outcomes. Similar analyses were conducted for other parameters of interest (i.e., the Dynamic Still Water Level (DWL), the Total Water Level (TWL), and Extent of Shoreline Retreat).

Consistent with results reported elsewhere (e.g., Woodworth and Blackman, 2004; Menéndez and Woodworth, 2010; Tebaldi, 2012; Obeysekera and Park, 2013; IPCC 2013), changes in flood magnitude track mean sea level trends - high tides and storms will ride the rising seas. For the future regional sea levels used here, changes in flood magnitude over the next 30 years or so are relatively small, on the order of one to two-thirds of a meter (1-2 feet), regardless of the GMSL scenario. Where effects are most likely to be felt is changes in flood frequency. Owing to the nature of the factors affecting coastal flooding along this segment of shoreline, increases on the order of 10 or 20cms in water level elevation were found to correspond to considerable changes in the projected return interval - from once a week to once a year, or from once a year to once a century. Thus, while 'major' floods are unlikely to change significantly in terms of frequency and magnitude, the frequency of 'minor' floods (~0.3m or 1 foot above MHHW) is expected to increase dramatically under all GMSL scenarios. What were relatively rare events will quickly become relatively common. Similar observations have been reported elsewhere (Sweet and Marra, 2014, 2015).

## Background

Elevated sea levels result from the complex interplay of a spectrum of oceanic, atmospheric, and terrestrial processes (Figure 1). The total water level (TWL) spectrum can be divided into three principal components: 1) fluctuations at the highest frequencies associated with local wave runup (e.g., setup

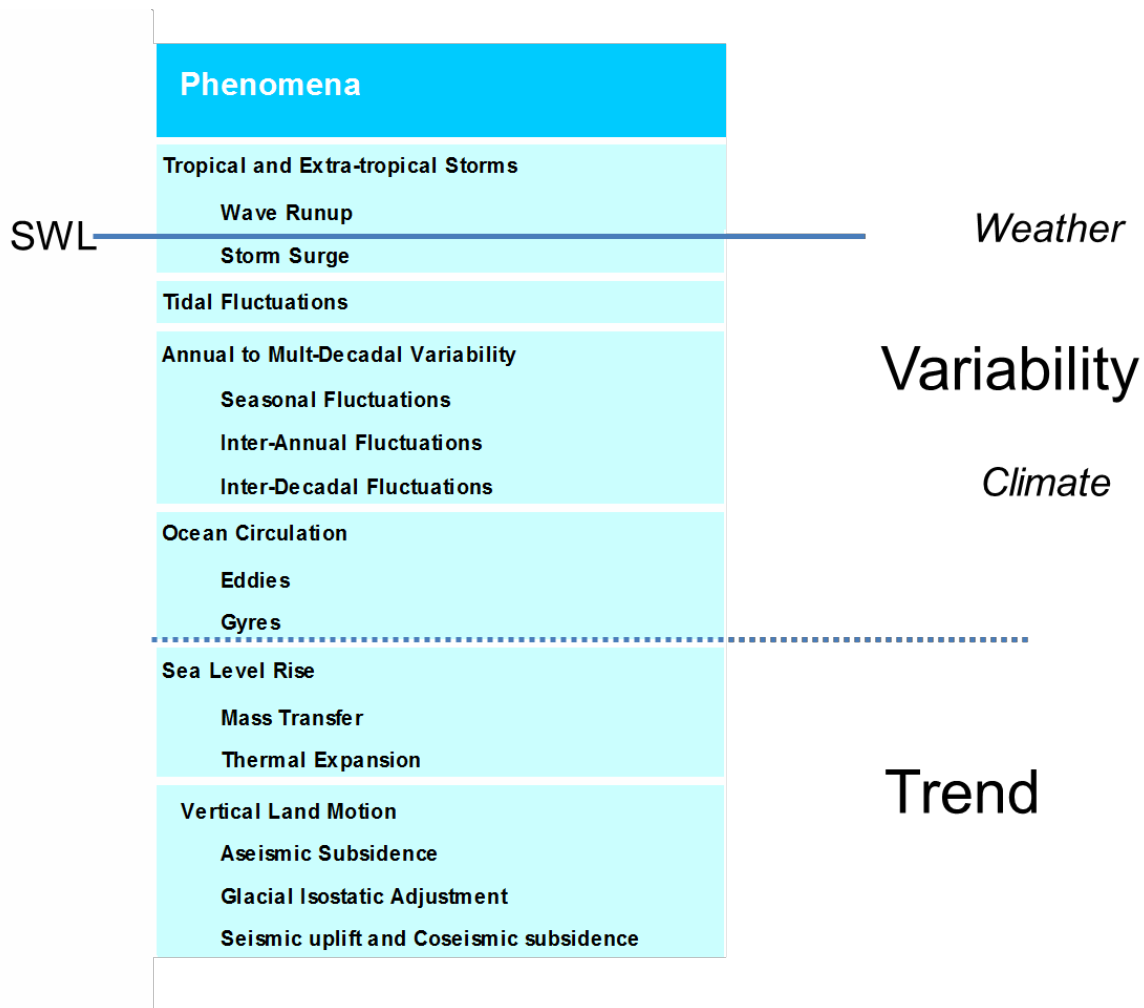


**Figure 1. Total Water Level (TWL) Spectrum** (after Marra et al., 2012). At one end of the spectrum are variations in elevation associated with the passage of surface gravity waves (e.g., wave runup). These high-frequency (seconds to minutes) variations are superimposed upon lower frequency (i.e., hourly to daily) variations in elevation attributable to phenomena such as tides and storm-induced surge. These elevation changes, in turn, rest upon other effects primarily related to variations in wind strength and ocean circulation that affects elevations at even longer time scales (i.e., weeks to decades). At the other end of the spectrum are isostatic and cryospheric variations (i.e., over centuries and millennia) linked to global Sea Level Rise (SLR). Vertical Land Motion (VLM) due to Glacial Isostatic Adjustment (GIA) or at a more local scale subsidence due to ground water extraction, for example, is also an important consideration in some settings. Still Water Level (SWL) refers to the combination of all these components with the exception of those at the highest frequencies associated with wave runup (e.g., setup plus swash). Note that the SWL is generally accepted as the parameter recorded by tide gauges since their placement and design generally minimizes wave effects.

plus swash); 2) fluctuations across a broad range of frequencies from local storm surge through to regional natural variability associated with patterns of atmospheric and oceanic circulation; and 3) fluctuations at the lowest frequencies associated with regional and global changes in absolute sea level and vertical land motion. Traditionally, the combination of components 2) and 3) are referred to as the Still Water Level (SWL). Here, the higher frequency components 2) are treated as 'Variability', and further subdivided into astronomical Tidal versus Non-Tidal Residual (NTR) components, where the NTR contains both weather-related components associated with tropical and extra-tropical cyclones and climate-related components associated with seasonal to inter-decadal variability. Lower frequency components 3) are treated as Trends and associated with the Mean Sea Level (MSL). This depiction is consistent with previous work and has been found to have broad application in the context of Extreme Value Analysis (EVA) and other statistical techniques related to assessing the likelihood of occurrence of extreme sea levels (e.g., Pugh 1987; Pugh 2004; Haigh et al., 2010; Haigh et al., 2013a; Haigh et al., 2013b; Merrifield et al., 2013).

It is well recognized that wave-driven inundation events are a major concern. The impact of wave-driven processes is twofold - breaking waves cause water levels to rise (wave setup) at the shoreline in some cases by 20- 30% of the breaking wave height, and energetic wave motions including harbor seiche can lead to inundation and flooding. Wave impacts vary with local topography, particularly with the presence of coral reefs, which significantly reduce wave energy. Flooding and erosion impacts will also vary with the elevation of the groundwater table and rates of precipitation. Thus it is important to understand the contribution of TWL (not just the SWL) as this has the potential to significantly alter spatially and temporally varying patterns and trends of coastal flooding.

## Study Area and Data Sources

An analysis of the potential impacts of sea level rise (SLR) on coastal flooding and shoreline retreat was conducted along a segment of shoreline on the Island of Hawai'i that extends from Kawaihae on the north to Kailua-Kona on the south (Figure 2). Results of the SWL and dynamic still water level (DSWL) analysis discussed below apply to this entire segment of shoreline. Results of the TWL and shoreline retreat analysis apply only to limited area of shoreline, the west-facing beaches that front the Kiholo and 'Aimakapā fishponds. Both are relatively steep beaches, with the gravel beach at Kiholo being smaller and narrower than the expansive stretch of sand beach at 'Aimakapā (Figure 3). Both beaches are subjected to North Pacific swells in the winter and South Pacific swells in the summer. However there is significant blockage and thus reduction in nearshore wave heights because of the main Hawaiian Islands northwest of the Big Island, (Vitousek, et al., 2010). Tides are semi-diurnal, with a mean range of 0.45m and diurnal range of 0.66m.

Data to support the analyses was collected from a range of field and lab-based sources. Ground control (horizontal and vertical) was established at multiple locations along the Kohala-Kona coast using CHC X90-OPUS (GPS) receivers over 7 days during September of 2015, with spot elevations and beach transects measured using a TopCon Total Station theodolite. In addition to being used for the flooding analyses per se, this information was used to rectify the 2013 USACE NCMP Topobathymetric Airborne

LIDAR data that formed the DEM used in this study. For the LIDAR topographic data Horizontal Positional Accuracy is compiled to meet 1m @ 95% confidence level and Vertical Positional Accuracy 19.6cm @ 95% confidence level (10cm RMSE). Sea level data was obtained from the NOAA tide gauge at Kawaihae Harbor, as well as other NOAA tide gauges in the Hawaiian Islands. Wave data was obtained from NOAA's buoys #51001 and #51101. Results reported in Vitousek et al. (2010) were also used to supplement this wave and water level information.

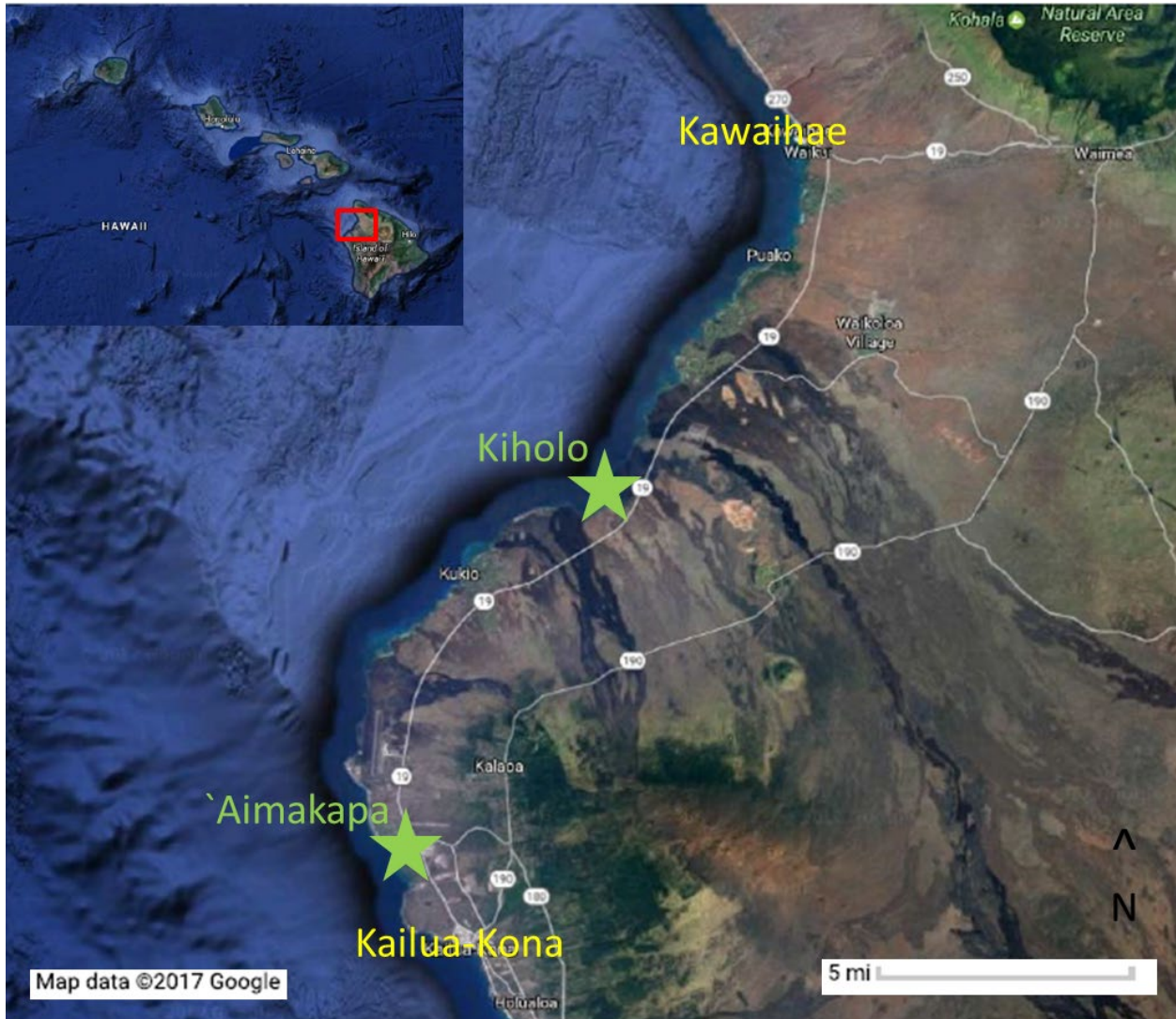


**Figure 2. Study Area.** The study area extends along the Kohala-Kona coast of the Island of Hawai'i, from Kawaihae on the north to Kailua-Kona on the south. More extensive data collection and analysis was carried out along the shoreline at Kiholo and 'Aimakapā (see text for details).

## Methodology

Overall, the approach taken here can be described as scenario or “risk-based” (e.g., Ruggiero, et al., 2001; Obeysekera and Park, 2013, Sweet et al., 2017). That is, different sources of data are used and different types of analyses are conducted so as to generate a range of results at different time periods

that are within scientifically plausible bounds. High or low end, less or more likely estimates, “best or worst case” scenarios if you like, can be selected from within this bracketed range of projected future conditions as can values in the middle of this range and that often reflect a convergence of results.

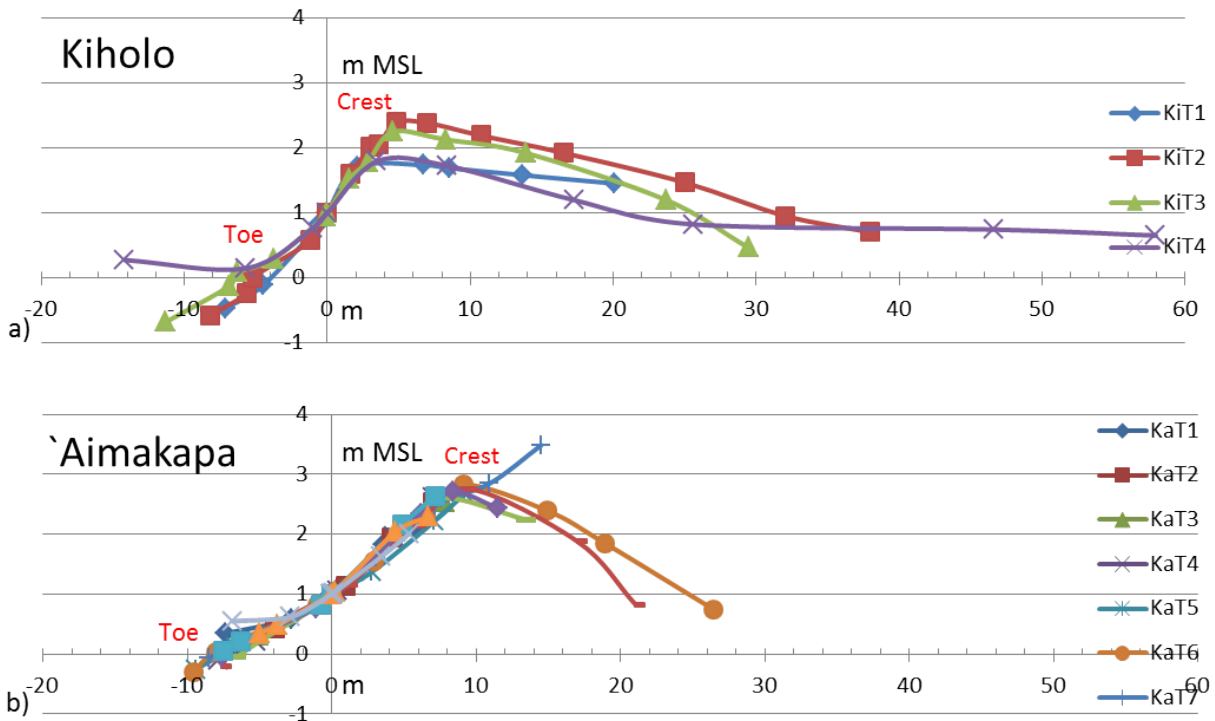


**Figure 3. Beach Profiles at a) Kiholo and b) 'Aimakapā.** Distance and elevation are in meters, with the latter relative to Mean Sea Level (MSL). The 1m elevation contour is identified as the mid-beach slope. Not the elevations of the beach crest at each location, as well as the differences in beach width and slope.

Two basic types of analysis were conducted as part of this study: 1) Analyses of flood extremes derived from a GEV distribution; and 2) Analyses of flood frequencies derived from a normal distribution. Details about these methods are considered below. Attention is then given to how these results were used to establish the plausible range in changes in the SWL, the DWL, the TWL, and Extent of Shoreline Retreat at different time periods, including instances where the results of these analyses were used in combined with those from previous work.

## Analysis of Flooding Extremes

### Stationary EVA

The prediction of the probability of exceeding a certain extreme sea level is useful for assessing current and future risk exposure (e.g., Marbaix and Nicholls, 2007; Obeysekera and Park, 2013), and employing various types of EVA to estimate extreme sea levels from tide gauge records is common practice (e.g., Coles 2001; FEMA 2005; Stephens 2012). A widespread approach to compute the extreme value statistical distributions is the GEV distribution. Three parameters characterize the cumulative distribution function given as:

$$G(x) = \begin{cases} \exp \left\{ - \left[ 1 + \xi \left( \frac{x - \mu}{\psi} \right) \right]_+^{-1/\xi} \right\} & \text{for } \xi \neq 0 \\ \exp \left\{ - \exp \left[ - \left( \frac{x - \mu}{\psi} \right) \right] \right\} & \text{for } \xi = 0 \end{cases}$$

where  $[a]_+ = \max [a, 0]$ ,  $\mu$  is the location parameter that specifies where the distribution is centered;  $\psi$  is the scale parameter which represents the dispersion, or spread of the extremes; and  $\xi$  is the shape parameter that determines the shape of the upper tail of the distribution, with  $\xi > 0$ ,  $\xi < 0$ , and  $\xi = 0$  defining Fréchet, Weibull, and Gumbel members of the GEV family respectively (Figure 4). The method selected to fit the data to the distribution is important. Block maxima used by the GEV can be annual or monthly. Most common is the Annual Maxima Method (AMM), where the GEV distribution is fitted to the sea-level annual maxima. Monthly block maxima provide further resolution into intra-annual variability as well as climatic co-dependence (Méndez et al. 2007). In the R-Largest Method (RLM), the GEV distribution is fitted to the  $r$  largest sea levels within the year, for a small number of  $r$  values in a year.

Much of the attention with respect to future estimates of extreme sea levels has focused solely on accounting for sea level rise. A commonly used approach involves generating the stationary extremes distribution using direct forms of EVA, and then creating a future estimate of extreme levels by simply adding back in the historically observed trend and/or sea level rise scenarios (e.g., Zervas, 2005; Tebaldi et al., 2012; Zervas, 2013). We used this same approach on Kawaihae tide gauge (Table 1). The hourly observed time series was downloaded from the University of Hawaii Sea Level Center (UHSLC) fast delivery database. The time series for this updated report extended to January 2018 and was not corrected for the inverse barometric effect. This timeseries includes a series of exceptional high tide events that occurred in 2016 and 2017. The detrended annual maxima water levels relative to Mean Higher High Water (MHHW) were analyzed using the AMM of GEV. The results was a range of return-interval estimates (e.g. 5-year, 25-year, and 50-year) for SWL at the Kawaihae tide gauge.

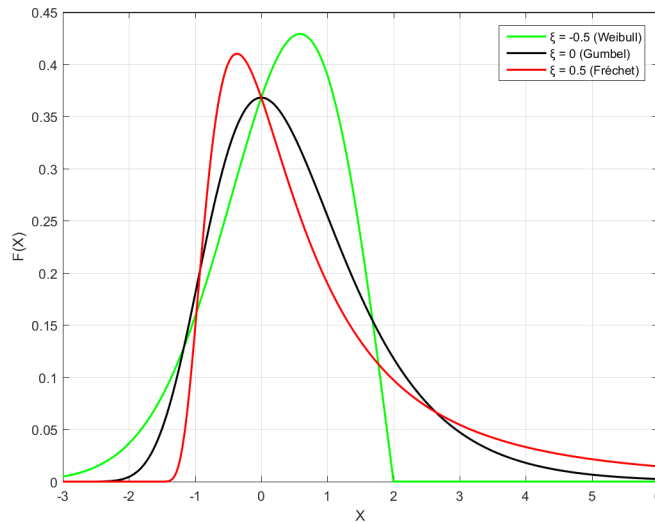


**Figure 4. Generalized Extreme Value (GEV) probability distribution function.** Location parameter is 0 and scale parameter is 1.

### Regional Frequency Analysis

Limitations with respect to the calculation of exceedance probabilities of extreme water levels from tide station records are well recognized (e.g., Coles, 2001; FEMA, 2005; McInnes et al., 2009; Thompson et al., 2009; Haigh et al., 2013a; Haigh et al., 2013b). They center on the issue of the extent to which any given station record is truly representative; for example, of sufficient length and, in particular, a length to accurately capture low probability events attributable to tropical cyclones. Because Kawaihae station only has 29 years of observations, Regional Frequency Analysis (RFA) from similar stations can minimize bias due to record length (Hosking and Wallis, 1997). RFA is a common approach in hydrology, but it is increasingly used in tide gauge analyses (Hall et al. 2016, Bardet et al. 2011, Barnadara et al. 2011). In RFA, data from different stations are combined with the assumption that the frequency distribution at each station is similar. A heterogeneity “H” score determines the homogeneity of different data stations. Once the stations are selected, a local scaling factor (“index event”) is used to pool the data from different stations and then analyzed using EVA. Based on the “H” score, the stations in Table 1 were considered homogeneous and used in RFA. The index event for each station is the mean of the

Station	# Years	First Year	Last Year*
HONOLULU	113	1905	2018
NAWILIWI	34	1954	2018
KAHULUI	68	1950	2018
HILO	91	1927	2018
KAWAIHAE	29	1989	2018

\*January is the only month from 2018 included in this analysis

**Table 1. Tide Gauge stations used in SWL analysis.** Hourly time series were obtained from the University of Hawaii Sea Level Center (UHSLC) fast delivery database.

observed annual maximum values. Each time series was divided by its index event and combined into one time series. The time series was then analyzed using a stationary AMM of GEV. We used this approach to generate another estimate of extreme sea levels along the Kohala- Kona coast.

### Non-Stationary EVA

Perhaps the biggest concern with the approaches considered above is their failure to account for changes in extreme event likelihood associated with patterns of sea level variability and storminess (as well as trends). As a result potential changes in the extremes distribution over discrete periods of time may in some cases be considerably under (or over) estimated. Similarly, changes in the extremes distribution over time due to changes in storm frequency (from changing storm tracks) for example, may also result in under (or over) estimation of the impacts of higher sea levels. The time varying approaches employed by Mendez et al. 2007, Menéndez et al. 2009, and Menéndez and Woodworth 2010 among others, that fit a GEV model to monthly tide station maxima so as to decipher long-term tidal cycles, intra-annual seasonal cycles and covariability with climate patterns as well as trends, can be used to address some of these concerns and generate products that provide a more accurate assessment of potential impacts due to extreme water levels in a changing climate. We applied these approaches to the Kawaihae tide station data to generate yet another estimate of sea level (i.e., SWL) extremes. We

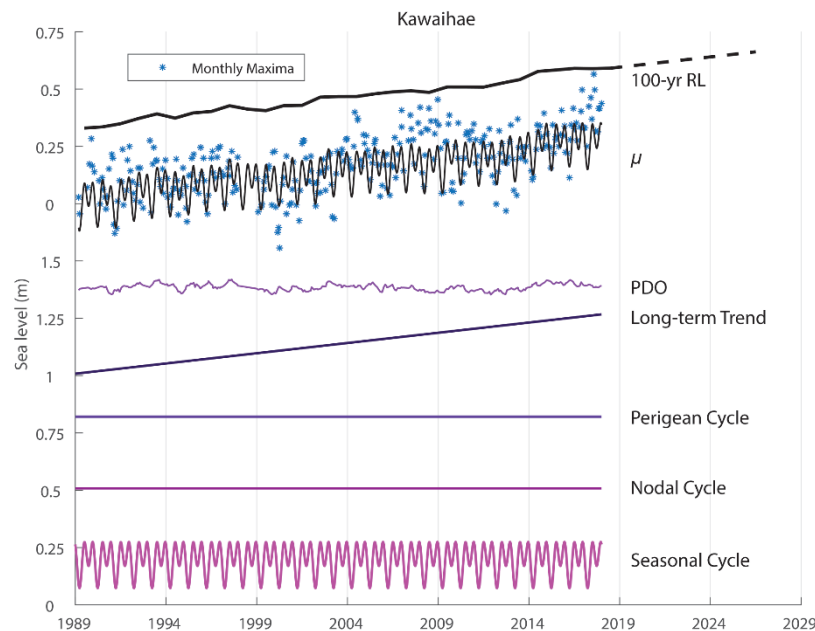


**Figure 5. Decomposition of extreme SWL at Kawaihae tide station.** Monthly maxima (blue asterisks) data are analyzed using a non-stationary GEV analysis. The location parameter ( $\mu$ : identifies where the distribution is centered) is decomposed into various components. For Kawaihae, the extreme signal is decomposed into intra-annual seasonal cycles, long-term tidal cycles (not significant in this run), and a long-term linear trend. Decomposition of covariability with climate patterns such as PDO was also assessed. The resulting 100-year return level incorporates these patterns and fluctuates with time.

used monthly maxima without the trend removed and decomposed the extreme signal into the seasonal cycle, perigean and nodal (tidal) cycles, and the long-term trend (Figure 5). We also assessed the change in extremes due to climate variability, using the Pacific Decadal Oscillation (PDO) as a covariate in the extremes model.

### SWL Scenarios

The three different analyses described above generated a range of results that were used to establish a set of “current” (2010) values for SWL elevations at different (high, medium, low) return intervals. In this document we used the Sweet et al. (2017) updated global mean sea level rise scenarios with the most recent research at the time on ice melt in Greenland and Antarctica and produced 1-degree gridded regionally-adjusted sea level change projections for the United States and its territories. Each gridded position has six SLR scenarios starting from Low (0.3m rise by 2100) and ending at Extreme (2.5m by 2100). SLR scenarios were also produced at locations of TGs along the U.S. coastline. All SLR scenarios account for oceanographic factors, changes in Earth’s gravitational field and rotations, flexure of the crust and upper mantle, melting of land-based ice, vertical land movement, and other non-climatic factors. We used values associated with the Intermediate-Low (0.5m), Intermediate (1.0m), and Intermediate-High (1.5m) scenarios for the Kawaihae tide gauge projections in our analysis. In some cases we added what amounted to a very small amount of sea level (0.05m) to the combined extreme plus sea level rise values to account for observations from the non-stationary GEV analyses which suggested there is a small amount of sea level change attributable to sea level variability (associated with the PDO) that could at any time occur in conjunction with sea level rise attributable to global warming. The projected SWL scenarios resulting from this analysis are considered further below.

### Dynamic Still Water Levels

Tide gauges are generally positioned at the ocean-land interface in protected waters and are covered by protective walls that dampen water level oscillations with periods  $\leq 5s$  (Sweet et al., 2015). Tide gauge measurements are collected every second for 3 minutes within a 6 minute segment. The SWL hourly measurement is the mean of all segments within the hour. Averaging the segments removes the high frequency signal in the data. Sweet et al. (2015) proposed using the standard deviation of the segments (i.e., sigma) to capture this high frequency. They showed that sigma estimates incident (wind and swell waves) and infragravity wave variability and is correlated to significant wave height. Adding the sigma to SWL in the following equation produces a dynamical water level (DWL) that contains a wave component:

$$DWL = SWL + \alpha * \sigma$$

where  $\alpha$  is the exceedance duration coefficient (i.e., 1.96 approximates the 95% of the Gaussian distribution). We used sigma for Kawaihae and fit this wave component with a stationary GEV (AMM) to generate values of DWL return intervals with an  $\alpha = 1.96$ .

Our assumption was that the DWL observed in the tide gauge was comparable to wave setup (a component of wave runup – see below). We compared our values to those calculated for wave setup by

Vitousek et al. (2010) using the dynamical Simulating Waves Nearshore (SWAN) model, and found them to show reasonable agreement across a range of return intervals. As a result we used the range of values generated by the two analyses to select a set of values for 'projected setup' under various scenarios and added this to the projected SWL values. As was the case with SWL we also used a non-stationary GEV analyses to estimate the amount of sea level change attributable to sea level variability (associated with the PDO) and in some cases added this to the combination of SWL and setup values. The projected DWL scenarios resulting from this analysis are considered further below.

### Wave Runup and TWL

Estimates of SWL (or DWL for that matter) do not fully capture the potential for coastal flooding. To do so requires an assessment of the TWL, the sum of SWL and wave-induced runup (e.g., Komar et al., 1999; Ruggiero et al., 2001; Mull and Ruggiero, 2014). Together with beach slope they determine the maximum inland extent of ocean incursion. Wave runup is itself the sum of setup and swash (Figure 6). Setup is the increase in water levels nearshore due to waves and swash (and backwash) is the layer of water that moves up (and down) the beach.

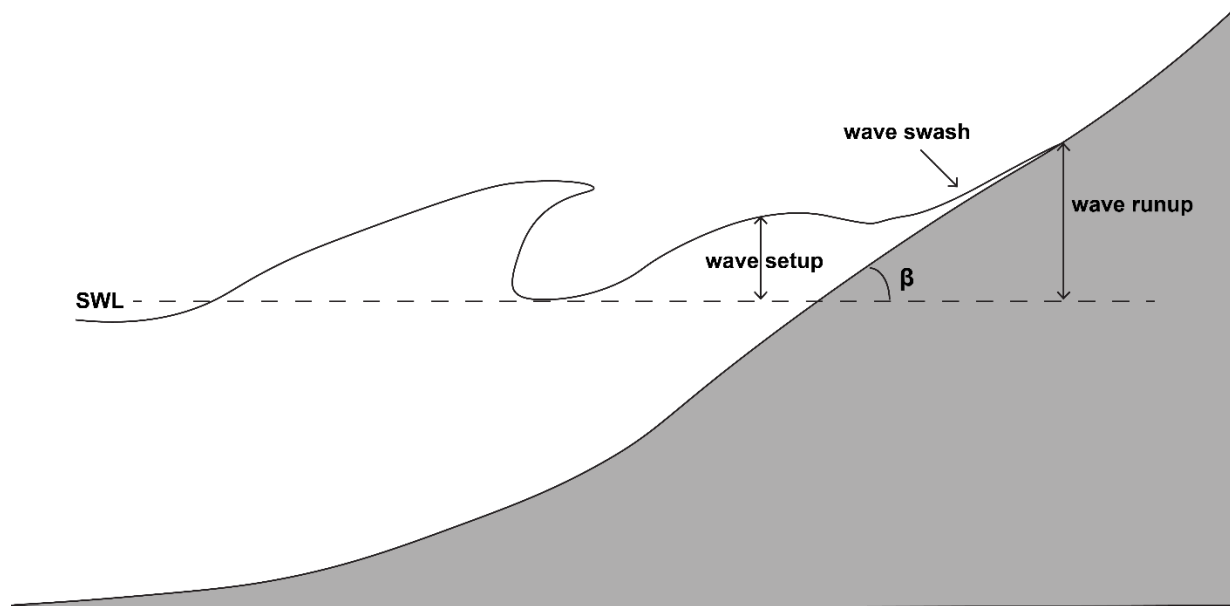


**Figure 6. Schematic of TWL.** TWL is SWL plus wave runup. Wave runup is the sum of wave setup plus swash;  $\beta$  is the slope of the beach and it, along with beach composition, has as an important influence on the inland extent of flooding. Adapted from Komar et al (1999).

To quantify the maximum extent of TWL, Stockdon et al. (2006) introduced a 2% exceedance of extreme wave runup height ( $R_2$ ) that takes into account deep-water significant wave height ( $H_0$ ), deep-water wavelength ( $L_0$ ) and foreshore slope ( $\beta_f$ ).

$$R_2 = \langle \eta \rangle + S$$

$$R_2 = 1.1 \left( 0.35\beta_f(H_0L_0)^{1/2} + \frac{[H_0L_0(0.563\beta_f^2 + 0.004)]^{1/2}}{2} \right)$$

This formula includes both setup ( $\langle\eta\rangle$ ) and swash ( $S$ ). Vitousek et al. (2010) indicated Stockdon's et al. (2006)  $R_2$  equation did not take into account fringing reefs and suggested a modified  $R_2$  equation that uses SWAN model outputs for nearshore significant wave height ( $H_n$ ), wavelength ( $L_n$ ), and setup.

$$R_2 = \langle\eta\rangle + S$$

$$R_2 = \langle\eta\rangle_{SWAN} + 1.1 \left( \frac{0.75\beta_f(H_nL_n)^{1/2}}{2} + 0.15H_0 \right)$$

In a study conducted along the same segment of shoreline considered here, Vitousek et al. (2010) used probability exceedance levels of  $H_0$  as boundary conditions to compute the nearshore output model outputs from SWAN. To assess probability exceedances for  $H_0$ , Vitousek et al. (2010) determined the largest wave heights affecting the Kohala coast occurred within the swell window 282°-305°. They selected data within this window and applied AMM to assess exceedance for deep-water wave using the top three significant wave heights per year. Because Hawai'i Island is sheltered by neighboring islands, wave exposure is reduced. Based on the SWAN model outputs, the effect of island blockage is accounted for as a 20% reduction in  $H_0$ . To model nearshore wave conditions and nearshore processes that result in further reductions in wave height at the shore (e.g., shoaling, refraction, convergence, and divergence) were also accounted for in SWAN (Vitousek et al., 2008).

Because of the relatively short length of the record in combination with the directional swell window used by Vitousek et al. (2010), as well as the inclusion of three maxima per year in their analysis (which increases the possibility of including non-extremes into the analysis), it is our belief that the return interval runup values they generated are under-estimates of what could actually occur. To address this concern, we conducted a corollary analysis using significant wave heights from deep-water buoys northwest of Kauai. We combined data from two buoys (NDBC buoy #51001 is 170 NM northwest of Kauai and #51101 is 190NM northwest of Kauai, Figure 7) using overlapping years to correct for any offsets. The resulting time series spans over 30 years (1981-2004). We use a stationary AMM of GEV to calculate probability exceedances at 1-yr, 2-yr, 10yr, 25-yr, 50-yr, and 100-yr (e.g., a 50-yr exceedance is the probability a wave will exceed a threshold once in 50 years, and can also be expressed as a 50 year return interval).  $H_0$  values were reduced by 20% due to island blockage and  $H_n$  was calculated by applying a shoaling factor to  $H_0$  (after Vitousek et al., 2010). We then used Vitousek's et al. (2010) modified  $R_2$  equation and nearshore outputs from the SWAN model to calculate runup. In the case of our analysis, it is our belief that the return interval runup values we generated are over-estimates of what could actually occur, because we used non-directional significant wave heights (i.e., did not filter the record so that it included only waves within the swell window) and only one maxima per year to assess exceedance probabilities.

Consistent with the approach used throughout this effort, we used a combination of the results from the two analyses described above to create a set of projected runup values at different (high, medium, low) return intervals for Kiholo, blending the “low-end” Vitousek (et al.2010) values with our “high-end” values and selecting values that fall within the bounds of this range. We then add these runup exceedance estimates to the SWL scenario estimates to get TWLs. The projected TWL scenarios for Kiholo that are the result of this analysis are considered further below.



**Figure 7. A combined time series from buoy #51001 and #51101 was used to assess runup.** (photo from: <http://www.ndbc.noaa.gov/>).

There are other things to note with respect to the TWL analysis. Beach slope is an important factor – small changes in beach slope result in large changes in wave runup. We ran the analysis for the range of beach slopes observed at the two sites. We did the same for a range of wave periods. So, the range of runup values we selected from - our range of plausible outcomes - was greater than would be the case with varying wave heights alone. We considered the possibility that wave heights (in addition to sea level) might be changing in a changing climate. Here, our review of results from Storlazzi, et al. (2015), who prepared a report on future wave and wind projections for the United States and United States-Affiliated Pacific Islands, suggested that little to no change is likely in the waves reaching the study area in the foreseeable future. We also conducted a simple empirical validation, comparing the observed height of the beach crest at ‘Aimakapā with the projected TWL at a low exceedances (e.g. 1-5 year return intervals). The assumption was that the existing beach morphology was an accurate reflection of the conditions it is exposed to (as this author has found to regularly be the case). The results were in good agreement. Taking this a step further, at Kiholo, where the beach is composed of gravel, we needed to account for a reduction in runup due to percolation into the beach. There, we were able to measure runup (on a separate occasion) during a high wave event, run these conditions back through our analysis and compare what was predicted to what we observed. We also compared the observed crest height and TWL heights projected for low return intervals like we did for ‘Aimakapā. Through these empirical analyses we calibrated runup at Kiholo, deriving a correction factor of 0.75 that was applied to calculated runup at this location.

## Shoreline Retreat

An assessment of how far the shoreline/beach might migrate landward in response to the combined effects of sea level rise and storms was conducted using a ‘geometric’ model described in Komar et al. (1999). A modification of a model proposed by Bruun (1954), this “K99” model was developed to estimate erosion of beaches backed by foredunes along the Oregon coast. This model is currently used by the state of Oregon to determine coastal hazard zones (Mull and Ruggiero, 2014). A similar approach is being applied in the Sea Level Report being prepared for the Hawaii State Interagency Climate Adaptation Committee. This model assumes that the slope of the beach remains constant, such that the shoreline moves up this slope as the beach erodes landward. The landward extent of shoreline retreat is dependent on the elevations of the projected TWL and the toe of the dune (*dtoe*):

$$E_{K99} = \frac{(TWL - dtoe)}{\tan \beta}$$

In our analysis, we use the distance measured from mid-beach (i.e., 1m above MSL) instead of *dtoe*. Other assumptions in the model are that: the sediment budget is balanced (there is no net increase or decrease in the supply of sediment to the nearshore system); the duration that the beach is exposed to the conditions associated with the projected TWL is unlimited (there is enough time for all the possible erosion that could occur to occur); and the composition of the beach being eroded is constant (e.g., there is no point where erosion would stop because the runup encounters underlying bedrock).

## Analysis of Flood Frequency

One particularly important consequence from rising sea levels is the increased frequency of coastal flooding due to storms, tides, and other climatic forcings. The gap between mean sea level and a flood threshold decreases, allowing for smaller storm surges or the highest tides to exceed the flood level. Sweet et al. (2014) and Sweet and Park (2014) describe this type of chronic minor flooding as nuisance (tidal-related) flooding. These relatively frequent flood events are not considered part of the extremes found in the upper tail of a probability density function (PDF) and as a result, potential changes in minor flooding needs to be analyzed differently. If nuisance flooding should occur simultaneously with either rainfall or wind-forced storm surges, the result could be severe and considered ‘extreme’ (Sweet et al. 2014).

As sea levels rise, there is corresponding increase in the probability of exceeding a threshold, or ‘tipping point’ (e.g., MHHW or the elevation of a feature of interest such as the top of a sea wall or the base of a building foundation; Sweet and Park 2014). At Kawaihae, the annual probability of exceedance of MHHW from 1996 to 2015 increased from 3% to almost 16% (Figure 8). Similar to Sweet et al. (2014) and Sweet and Park (2014), based on an analyses of flood frequencies derived from a normal distribution we calculated the number of days in a year the daily maximum SWL exceeded a nuisance threshold for a range of regionally adjusted sea level rise projections. The nuisance threshold varied in increments of 10 cm starting at MHHW and ending at MHHW + 2.6 m. We used regionally adjusted scenario-based sea level rise projections from Sweet et al. (2017) (see above) to project the annual number of days the SWL exceed a given flooding threshold (Figure 9). The low, medium, and high

scenarios correspond to Intermediate-Low, Intermediate, and Intermediate-High SLR scenarios. In addition to the sea level projections, we used historical observations without any future sea level adjustments and identify this as our LOW projections (see Sweet and Park 2014 for more information).

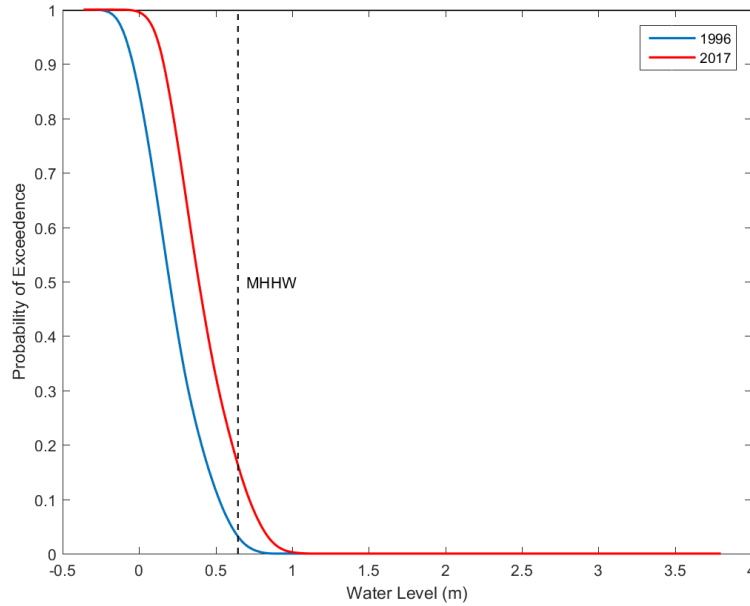


**Figure 8. Probability of exceedance for annual records of hourly water levels at Kawaihae tide gauge.**

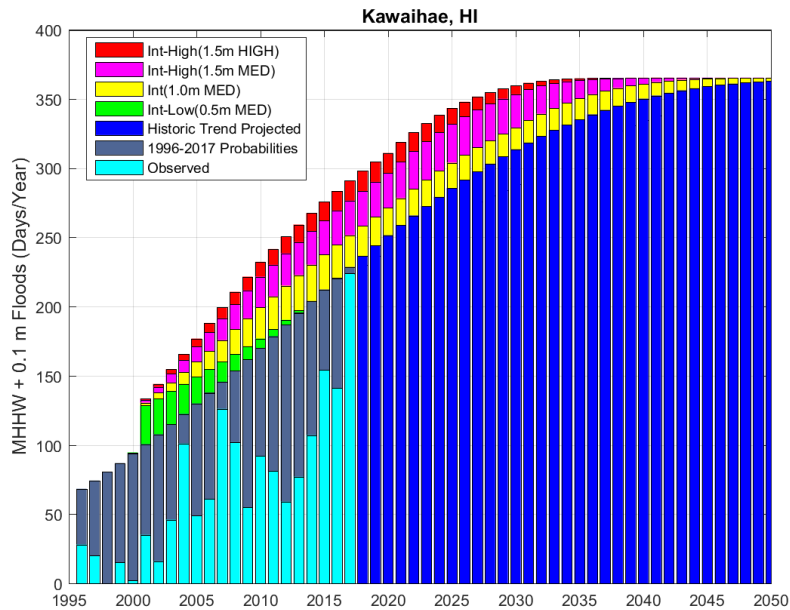


**Figure 9. Nuisance floods exceeding MHHW+0.1m at Kawaihae tide gauge.**

## Results

Results of the various analyses described above are described below and summarized in the Tables that follow.

### SWL Scenarios

Table 2 shows the potential magnitude of the SWL (in m above MHHW) for a range of flood scenarios for the time periods 2030, 2040, 2050, 2080, and 2100. In terms of flood frequency (or return intervals) the LOW, MEDIUM, and HIGH scenarios correspond to roughly once every 1-2 years, once every 25-50 years, and once every 100plus years. Details about the derivation of these values are provided above. Extreme Value Return Intervals are 0.3m, 0.4m, and 0.5m (above MHHW) for low, medium, and high scenarios respectively. In our assessment of extreme SWL, RFA analysis and the analysis from Kawaihae we found result to be quite similar. For example, the 2-yr return level (also referred to as 2-yr storm: the probability a water level can reach this elevation once in 2 years) at Kawaihae of 0.3m above MHHW is similar to the 2-yr return level (0.31m) with RFA. RFA results are slightly higher as the return periods increase (2-yr storm to 100-yr storm). For example, the 100-yr storm for Kawaihae is 0.42m and RFA is 0.50m. Bringing in other tide gauges is probably a better indicator of potential exposure than relying solely on the results from one tide gauge. Hence, we selected the higher value. The non-stationary results (see Figure 5) tend to site somewhere between, having higher water levels at lower return periods (2-yr storm = 0.38m) and lower water levels at higher return periods (100-yr storm = 0.46m) compared to the stationary analyses. What is particularly noteworthy is that in all cases the maximum difference between a 2-yr storm and a 100-yr storm is quite small - around 20cm.

Scenarios		Extreme Value Return Level (m)	SLC trend (Sweet et al. 2017) (m)	Climate Variability (m)	Projected SWL Value (m) MHHW
2030	LOW	0.3	0.2	0	0.5
	HIGH	0.5	0.28	0.05	0.8
2040	LOW	0.3	0.27	0	0.6
	MEDIUM	0.4	0.35	0.05	0.8
	HIGH	0.5	0.43	0.05	1.0
2050	LOW	0.3	0.34	0	0.6
	MEDIUM	0.4	0.48	0.05	0.9
	HIGH	0.5	0.62	0.05	1.2
2080	LOW	0.3	0.56	0	0.9
	MEDIUM	0.4	0.95	0.05	1.4
	HIGH	0.5	1.36	0.05	1.9
2100	LOW	0.3	0.72	0	1.0
	MEDIUM	0.4	1.36	0.05	1.8
	HIGH	0.5	2.03	0.05	2.6

**Table 2. SWL Scenarios.**

Sea level trends applied here increase that range from 20cm by 2030 (from 2010 ‘current’ conditions) to just over 2m by 2100. An important point to note is that the magnitude of sea level change over the next 30 years or so is relatively small and the spread in value is quite narrow, on the order of one to two-thirds of a meter (1-2 feet) - regardless of which GMSL scenario is selected (and this includes those of Sweet et al., 2017). It takes some time for the effects of acceleration to be fully realized.

When all factors are considered - flood extremes, future regional sea levels and possible contributions attributable to climate variability, changes in the projected SWL (m relative to MHHW) range from 0.5-0.8m by 2030, from 0.6-1.0m by 2040, from 0.6-1.2m by 2050, from 0.9-1.9m by 2080, and from 1.0-2.6m by 2100.

Scenarios		Projected SWL Value (m)	Projected "setup" (m)	Climate Variability (m)	Projected DSWL Value (m) MHHW
2030	LOW	0.5	0.4	0	0.9
	HIGH	0.83	0.8	0.17	1.8
2040	LOW	0.57	0.4	0	1.0
	MEDIUM	0.8	0.6	0.17	1.6
	HIGH	0.98	0.8	0.17	2.0
2050	LOW	0.64	0.4	0	1.0
	MEDIUM	0.93	0.6	0.17	1.7
	HIGH	1.17	0.8	0.17	2.1
2080	LOW	0.86	0.4	0	1.3
	MEDIUM	1.4	0.6	0.17	2.2
	HIGH	1.91	0.8	0.17	2.9
2100	LOW	1.02	0.4	0	1.4
	MEDIUM	1.81	0.6	0.17	2.6
	HIGH	2.58	0.8	0.17	3.6

**Table 3. DWL Scenarios.**

### DWL Scenarios

Table 3 shows the potential magnitude of the DWL (in m above MHHW) for a range of flood scenarios for the time periods 2030, 2040, 2050, 2080, and 2100. Each of the scenarios reflect a combination of the projected SWL (in Table 2) and an increase above SWL associated with wave “setup”. They may also include a small contribution attributable to climate variability. When all factors are considered, changes in the projected DWL (m relative to MHHW) range from 0.9-1.8m by 2030, from 1.0-2.0m by 2040, from 1.0-2.1m by 2050, from 1.3-2.9m by 2080, and from 1.4-3.6m by 2100. This ‘DWL’ estimate is rather novel and unique. It is provided here as a way to get a better sense of the potential for coastal flooding beyond that which is provided by the SWL alone. It includes some, but not all of the ‘extra’ flooding induced by waves. Unlike the TWL, owing to its linkage to beach slope, is highly localized, the DWL has broader regional application, for example, by providing a buffer on the potential exposure to flooding that extends beyond that provided by SWL.

## TWL Scenarios

Table 4 shows the potential magnitude of the TWL (in m above MHHW) for a range of flood scenarios for the time periods 2030, 2040, 2050, 2080, and 2100 at Kiholo. Each of the scenarios reflect a combination of the projected SWL (in Table 2) and an increase above SWL associated with wave “runup”. Differences in runup values at each site are attributable to differences in projected wave heights and periods associated with each scenario. We used three runup values for our TWL calculations. The <10-yr storm waves (2.06 m) is based on Vitousek et al. (2010) results. The 10-50-yr storm wave (2.40 m) is based on the high-end estimate of Vitousek et al. (2010) and the low-end estimate of our runup analysis, and the 50-100-yr storm wave (2.57 m) is based on our runup analysis. Differences in runup values between the two sites (for similar wave conditions) are the result of differences in beach slope and the material that composes the beach. Details about the derivation of these TWL estimates are provided above.

When SWL and runup are combined, changes in the projected TWL (m relative to MHHW) range from 2.6-3.4m by 2030, from 2.6-3.6m by 2040, from 2.7-3.7m by 2050, from 2.9-4.5m by 2080, and from 3.1-4.5.2m by 2100 for Kiholo (Table 4).

Scenarios		Projected SWL Value (m) MHHW	Projected Runup Value (m)	Projected TWL Value (m) MHHW
2030	LOW	0.50	2.06	2.6
	HIGH	0.83	2.57	3.4
2040	LOW	0.57	2.06	2.6
	MEDIUM	0.8	2.40	3.2
	HIGH	0.98	2.57	3.6
2050	LOW	0.64	2.06	2.7
	MEDIUM	0.93	2.40	3.3
	HIGH	1.17	2.57	3.7
2080	LOW	0.86	2.06	2.9
	MEDIUM	1.40	2.40	3.8
	HIGH	1.91	2.57	4.5
2100	LOW	1.02	2.06	3.1
	MEDIUM	1.81	2.40	4.2
	HIGH	2.58	2.57	5.2

**Table 4. TWL Scenarios at Kiholo.**

## Shoreline Retreat Scenarios

Table 5 show the potential magnitude of shoreline retreat (in meters landward from the “mid-beach” – (0.624m above MHHW) for a range of scenarios for the time periods 2030, 2040, 2050, 2080, and 2100. What this means is that, assuming the existing beach morphology, this same form – the beach toe, mid-beach, and beach crest - will all migrate inland (and upward) as one by the given amount. Following

from the application of the ‘K99’ model, differences in projected retreat values among the scenarios are attributable to differences in projected TWL and beach slope. Beach slopes ( $\tan \beta$ ) used here ranged from 0.20 to 0.33 for Kiholo. Details about the derivation of these values are provided above.

When TWL and beach slope are combined, the projected landward retreat of the shoreline from its current position ranges 5.7-13.7m by 2030, from 5.9-14.5m by 2040, from 6.1-15.4m m by 2050, from 6.7-19m m by 2080, and from 7.2-22.3m m by 2100 for Kiholo (Table 5). It is interesting to note that these are fairly narrow bands of shoreline change, and further they do not vary considerably among the LOW and MEDIUM Scenarios. For example, across all time periods and using the LOW Scenario, the results suggest shoreline retreat will be at least 5-7m (~16 to feet inland) between now and 2100. For the HIGH Scenario, shoreline retreat will be at least 13-22m (~43 to 72 feet inland) between now and 2100.

Scenarios		Projected TWL Value (m) MHHW	Projected Retreat Distance* (m)
2030	LOW	2.56	5.7
	HIGH	3.4	13.7
2040	LOW	2.63	5.9
	MEDIUM	3.2	10.1
	HIGH	3.55	14.5
2050	LOW	2.7	6.1
	MEDIUM	3.33	10.6
	HIGH	3.74	15.4
2080	LOW	2.92	6.7
	MEDIUM	3.8	12.5
	HIGH	4.48	19.0
2100	LOW	3.08	7.2
	MEDIUM	4.21	14.1
	HIGH	5.15	22.3

**Table 5. Shoreline Retreat Scenarios at Kiholo.**

\* Distance measured from Mid-Beach (1m above MSL; 0.62m above MHHW)

## Flood Frequency

Table 6 shows the results of the flood frequency analysis, with the number of days a given elevation threshold is exceeded (i.e., 10cm increments starting at MHHW and ending at 2m above MHHW followed by 20 cm increments to 2.6m above MHHW) for a range of scenarios for the time periods 2030, 2040, 2050, 2080, and 2100.

Scenarios		Floods (Days/Year)										
		Threshold (m) = MHHW +										
		0	0.1	0.2	0.3	0.4	0.5	0.6	0.7	0.8	0.9	1
2030	LOW	347	288	188	85	22	2	0	0	0	0	0
	HIGH	364	353	303	210	103	30	4	0	0	0	0
2040	LOW	361	334	261	154	61	12	1	0	0	0	0
	MEDIUM	365	360	329	252	143	54	10	0	0	0	0
	HIGH	365	365	361	334	261	154	61	12	1	0	0
2050	LOW	364	357	317	232	123	41	6	0	0	0	0
	MEDIUM	365	365	363	343	279	176	77	18	1	0	0
	HIGH	365	365	365	365	360	329	252	143	54	10	0
2080	LOW	365	365	364	357	317	232	123	41	6	0	0
	MEDIUM	365	365	365	365	365	365	364	359	323	242	133
	HIGH	365	365	365	365	365	365	365	365	365	365	365
2100	LOW	365	365	365	365	361	334	261	154	61	12	1
	MEDIUM	365	365	365	365	365	365	365	365	365	365	364
	HIGH	365	365	365	365	365	365	365	365	365	365	365
Scenarios		Floods (Days/Year)										
		Threshold (m) = MHHW +										
		1.1	1.2	1.3	1.4	1.5	1.6	1.7	1.8	2	2.2	2.4
2030	LOW	0	0	0	0	0	0	0	0	0	0	0
	HIGH	0	0	0	0	0	0	0	0	0	0	0
2040	LOW	0	0	0	0	0	0	0	0	0	0	0
	MEDIUM	0	0	0	0	0	0	0	0	0	0	0
	HIGH	0	0	0	0	0	0	0	0	0	0	0
2050	LOW	0	0	0	0	0	0	0	0	0	0	0
	MEDIUM	0	0	0	0	0	0	0	0	0	0	0
	HIGH	0	0	0	0	0	0	0	0	0	0	0
2080	LOW	0	0	0	0	0	0	0	0	0	0	0
	MEDIUM	47	8	0	0	0	0	0	0	0	0	0
	HIGH	363	347	288	188	85	22	2	0	0	0	0
2100	LOW	0	0	0	0	0	0	0	0	0	0	0
	MEDIUM	357	317	232	123	41	6	0	0	0	0	0
	HIGH	365	365	365	365	365	365	365	361	261	61	1

**Table 6. Flood Frequency.** Note that MHHW occurs ~180 days a year, or every other day. Also flood elevations are SWL values, so they do not include wave runoff. As a result, actual observed flood elevations are expected to be significantly higher.

What the results show is that regular, almost daily flooding (> 200 days/year) happens for elevations 10 to 30cm above MHHW by 2030, 10 to as much as 40cm above MHHW by 2040, 10 to as much as 60cm above MHHW by 2050, 10 to as much as 1.3m above MHHW by 2080, and 10 to as much as 2m above MHHW by 2100. Similarly frequent, weekly to monthly (~10 to 60 day/year) flooding happens for elevations 40 to 50cm above MHHW by 2030, 40 to as much as 70cm above MHHW by 2040, 50 to as

much as 90cm above MHHW by 2050, 70 to as much as 1.6m above MHHW by 2080, and 80 to as much as 2.2m above MHHW by 2100. Infrequent but not rare, roughly annual (3 to 1 day/year) flooding happens for elevations 50 to 60cm above MHHW by 2030, 60 to 80cm above MHHW by 2040, 80cm above MHHW by 2050, 1.7m above MHHW by 2080, and 2.4m above MHHW by 2100. Beyond this, recurrence intervals begin to blend with those estimated through the extremes analysis.

It is interesting to note how sensitive changes in frequency are to changes in sea level. A change of 20cm, whether it reflects a change within (the threshold) or between (sea level rise) any given scenario, can manifest as a dramatic difference in the number of flood days (days exceeding the threshold). For example, for 2030 a 20cm increase in the threshold (from 20 to 40cm above MHHW) corresponds to a roughly 5 fold difference in flood frequency. For 2080 at the 90cm threshold, the difference between the LOW and MEDIUM scenarios corresponds to a change from no flooding to flooding every day. A similar observation about how sensitive changes in frequency are to changes in sea level was made earlier in the context of extremes. This is indicative of what a narrow band of sea level change the area has historically experienced.

## Discussion

The results of the analysis presented here reflect updates to (1) timeseries the recent episodes of exceptional high tides and (2) updated regional sea-level rise projections of Sweet et al. (2017). As in the previous version, they are intended to serve multiple applications. A full discussion of such is beyond the scope of this document. Attention is briefly given to how the results presented here compare to those reported in previous studies of the same general study area – though principally the beach fronting the ‘Aimakapā fish pond - that also assess future flood and erosion potential.

Hapke, et al., (2005) conducted a study of coastal change at Kaloko-Honokōhau National Historic Park, an area that encompasses the beach fronting the ‘Aimakapā fishpond. A major part of their work was the analysis of shoreline change from 1950 to 2002 using aerial photographs. Average annual recession rates (AARs) were found to be variable along the segment of shoreline fronting the ‘Aimakapā fishpond and areas just north and south (the area considered in this study), ranging from -0.6 to -0.2m/year for areas north and south of the fishpond and < -0.1m/year for the area directly in front of the fish pond. The combined AAR for the entire study area was -0.3m.

For the time periods used in our study and the AARs from Hapke et al. (2015), landward retreat of the shoreline in 2030 (from 2010) is projected as 6m for the area average, and as high as 12m and as low as 2m using values elsewhere. For 2040, the average is 9m and the range is 18 to 3m. For 2050, the average is 13.5m and the range is 27 to 4.5m. For 2080, the average is 22.5m and the range is 45 to 7.5m. For 2100, the average is 27m and the range is 54 to 9m. Although we did not update ‘Aimakapā with the Sweet et al. (2017) scenarios, our previous version (using Kopp et al., 2015, and centering on the year 2005) did assess ‘Aimakapā, which had corresponding values of 12-20m by 2025, from 12-22m by 2035, from 13-22m by 2050, and from 14-26m by 2080. Without getting into a lengthy discussion about the limitations of AARS from aerial photographs, suffice it to say that that there is reasonable agreement between the results from the two different analyses. The AAR-based estimates tend to be

lower than the geometric-model based estimates during the early years and vice-versa for the later years, where the AAR-based estimates tend to be higher than the geometric-model.

The work of Vitousek et al. (2010) is noted in multiple instances above. Their work was very similar in nature to that presented here. Some of the differences between their work and the work presented here have already been highlighted (e.g., differences in wave climate estimates). Here the focus is on how their result compare to those of this study as far as future flood magnitude and frequency.

For the beach fronting the 'Aimakapā fishpond, Vitousek et al. (2010) report projected runup ranging from 1.97m to 2.54m for 5- to 50-year return intervals respectively. Here the projected runup for the corresponding range return intervals is 2.30 to 2.59m. Vitousek et al. (2010) do provide estimates of sea level rise, using values of plus 0.25, 0.5, and 1m. Their range is less than that used here, which range from 0.20 to 2.03m. However, unlike this study they do not provide explicit time periods associated with these estimates.

Vitousek et al. (2010) conducted an analysis of changes in flood frequency. Similar to what is reported here they noted that *“impacts to fixed structures (relative to a given threshold) do not increase linearly; they accelerate.”* They go on to suggest that beach fronting 'Aimakapā Fishpond at elevations > 2 m above MSL elevation) should be relatively resilient against overtopping impacts until sea-level rise scenarios greater than +0.5 m become reality. Using 2.25m above MSL as a threshold (assumed to correspond to the elevation of the beach crest at this location and consistent with our observation of such) they report an increase from 1 to 12 hours of overtopping per year for a 0.5m increases in sea level. Our results are not directly comparable because we expressed the changes in flood frequency in days per year (not hours). However, for the sake of discussion, using the Vitousek et al. (2010) 1-year runup estimate of 1.6m along with a corresponding value (0.48m MEDIUM by 2050) suggests overtopping of the beach crest would be an almost daily occurrence (at that elevation/by that time). Using our estimates, even by 2035 overtopping of the beach crest could occur as frequently as every other day.

Vitousek et al. (2010) also conducted an analysis of shoreline change from 1950 to 2002 using aerial photographs. For the beach fronting the 'Aimakapā Fishpond an average long term shoreline change rate (EX) of  $-0.3 \pm 0.1\text{ft/yr}$  (i.e.,  $-0.1\text{m/yr}$ ). This is consistent with results of Hapke, et al. (2005) reported above. Later, they suggest AAR along the beach fronting 'Aimakapā Fishpond is between 0.25-0.5ft/year, which corresponds to shoreline retreat on the order of 10-20 feet (3-6m) by 2050. This also falls within the bounds reported by Hapke et al. (2005). However these values are as little as one-half to as much as one-eighth as that predicted here using the geometric model.

## Conclusions

A series of analysis was conducted to assess the potential for flooding and erosion along a section of shoreline extending from Kawaihae to Kailua-Kona, on the Island of Hawai'i in response to projected changes in sea level due to global warming.

In general, results are consistent with those reported elsewhere (e.g., Woodworth and Blackman, 2004; Menéndez and Woodworth, 2010; Tebaldi, 2012; Obeysekera and Park, 2013; IPCC 2013), changes in flood magnitude track mean sea level trends - high tides and storms will ride the rising seas. For the future regional sea levels used here, changes in flood magnitude over the next 30 years or so are relatively small, on the order of one to two-thirds of a meter (1-2 feet) regardless of the GMSL scenario. Where effects are most likely to be felt is changes in flood frequency. Owing to the nature of the factors affecting coastal flooding along this segment of shoreline, increases on the order of 10 or 20cms in water level elevation were found to correspond to considerable changes in the projected return interval - from once a week to once a year, or from once a year to once a century. Thus, while 'major' floods are unlikely to change significantly in terms of frequency and magnitude, the frequency of 'minor' floods (~0.3m or 1 foot above MHHW) is expected to increase dramatically under all GMSL scenarios. What were relatively rare events will quickly become relatively common. Similar observations have been reported elsewhere (Sweet and Marra, 2014; and 2015).

Results compare favorably with previous work carried out by others in this area (i.e., Hapke et al., 2005; Vitousek et al. (2010), though projected SWL and TWL magnitudes presented here tend to be somewhat higher and shoreline retreat distances further inland than that suggested by previous studies (for comparable time frames). What is particularly unique about this work is that it does provide specific time frames for the estimates for projected changes. Also it provides an analysis of flood frequency that is particularly amenable to assessing potential risks to built and natural assets.

*The results presented here are presented in a risk-based construct that provides a range of scientifically defensible scenarios. Which scenarios should be selected depends both on the application and the level of risk deemed appropriate for that application. It is strongly recommend they be used in consultation with qualified professionals. They should not be used for siting and design purposes. They should be considered subject to modification in light of new information and/or improved techniques.*

## References

- Bruun, P., (1954). Coast erosion and the development of beach profiles. Beach erosion board technical memorandum No. 44. U.S. Army Engineer Waterways Experiment Station. Vicksburg, MS.
- Coles, S. G. (2001). An introduction to statistical modeling of extreme values. London: Springer, 208 pp.
- FEMA, (2005). Final Draft Guidelines for Coastal Flood Hazard Analysis and Mapping for the Pacific Coast of the United States.
- Haigh I., Nicholls R., Wells N. (2010). Assessing changes in extreme sea levels: Application to the English Channel, 1900–2006, *Continental Shelf Research*. doi:10.1016/j.csr.2010.02.002.
- Haigh, I.D., Wijeratne, E.M.S., MacPherson, L.R., Pattiaratchi, C.B., Mason, M.S., Crompton, R.P., and George, S. (2013a). Estimating Present Day Extreme Water Level Exceedance Probabilities Around the Coastline of Australia: Tides, Extra-tropical Storm Surges and Mean Sea Level. *Climate Dynamics*, published online 12 January 2013. Springer Verlag. DOI: 10.1007/s00382-012-1652-1.
- Haigh, I.D., Wijeratne, E.M.S., MacPherson, L.R., Pattiaratchi, C.B., Mason, M.S., Crompton, R.P. and George, S. (2013b). Estimating Present Day Extreme Water Level Exceedance Probabilities Around the Coastline of Australia: Tropical Cyclone-induced Storm Surges. *Climate Dynamics*, published online 01 February 2013. Springer Verlag. DOI :10.1007/s00382-012-1653-0.
- Hapke, C.J., R. Gmirkin, B.M. Richmond (2005). Coastal change rates and patterns: Kaloko-Honokōhau NHP, Kona Coast, Hawai'i. U.S. Geological Survey Open-file report 2005-1069. <http://pubs.usgs.gov/of/2005/2005-1069/>
- IPCC 2013. AR5 Synthesis Report. *Climate Change (2013). The Physical Science Basis. Contribution of Working Group I to the Fifth Assessment Report of the Intergovernmental Panel on Climate Change* [Stocker, T.F., Qin, D., Plattner, G.K., Tignor, M., Allen, S.K., Boschung, J., Nauels, A., Xia, Y., Bex, V. and Midgley P.M. (eds.)]. Cambridge University Press, Cambridge, United Kingdom and New York, NY, USA, 1535 pp.
- Komar, P.D., W.G. McDougal, J.J. Marra, and P. Ruggiero (1999). The rational analysis of setback distances: applications to the Oregon Coast. *Shore & Beach*, 67(1), 41-49.
- Kopp, R. W., R. M. Horton, C. M. Little, J. X. Mitrovica, M. Oppenheimer, D. J. Rasmussen, B. H. Strauss, and C. Tebaldi (2014). Probabilistic 21st and 22nd century sea-level projections at a global network of tide gauge sites, *Earth's Future*, 2,383–406, doi:10.1111/eft2.2014EF000239.
- Marbaix, P. and Nicholls, R. J. (2007). Accurately determining the risks of rising sea level. *Eos, Transactions of the American Geophysical Union*, 88, 441 – 442.
- McInnes, K.L., Macadam, I., Hubbert, G.D. and O'Grady, J.G. (2009). A Modelling Approach for Estimating the Frequency of Sea Level Extremes and the Impact of Climate Change in Southeast Australia. *Natural Hazards*, 51, 115–137.
- Meinshausen, M., S.J. Smith, K. Calvin, J.S. Daniel, M. L. T. Kainuma, J-F. Lamarque, K. Matsumoto, S.A. Montzka, S.C.B. Raper, K. Riahi, A. Thomson, G.J.M. Velders, D.P.P. van Vuuren (2011). The RCP

- greenhouse gas concentrations and their extensions from 1765 to 2300, *Clim. Change*, 109, 213-241, doi:10.1007/s10584-011-0156-z.
- Méndez, F. J., Menéndez, M., Luceño, A., and Losada, I. J. (2007). Analyzing monthly extreme sea levels with a time-dependent GEV model. *Journal of Atmospheric and Oceanic Technology*, 24(5), 894-911.
- Menendez, M., Mendez, F.J., and Losada, I.J. (2009). Forecasting Seasonal to Interannual Variability in Extreme Sea Levels. *ICES Journal of Marine Science*, 66, 1490–1496.
- Menendez, M., and Woodworth, P.L. (2010). Changes in Extreme High Water Levels Based on a Quasi-global Tide-gauge Data Set. *Journal of Geophysical Research*, 115(C10), C10011, DOI:10.1175/2011JCLI3932.1.
- Merrifield, M. A., A. S. Genz, C. P. Kontoes, and J. J. Marra (2013). Annual maximum water levels from tide gauges: Contributing factors and geographic patterns, *J. Geophys. Res. Oceans*, 118, 2535–2546, doi:10.1002/jgrc.20173.
- Mull, J. and P. Ruggiero (2014). Estimating Storm-Induced Dune Erosion and Overtopping along U.S. West Coast Beaches, *J. of Coastal Research*, 30(6), 1173-1187.
- Obeysekera, J. and Park, J. (2013). Scenario-Based Projection of Extreme Sea Levels. *Journal of Coastal Research*, 29(1), 1–7. January 2013. DOI: 10.2112/JCOASTRES-D-12-00127.1
- Pugh, D.T. (1987). *Tides, Surges and Mean-Sea Level*, John Wiley & Sons, Ltd., New York, New York.
- Pugh, D.T. (2004). *Changing Sea Levels: Effects of Tides, Weather and Climate*. Cambridge University Press, Cambridge, United Kingdom, 280pp.
- Ruggiero, P., P.D. Komar, W.G. McDougal, J.J. Marra, and R.A. Beach (2001). Wave Runup, Extreme Water Levels and the Erosion of Properties Backing Beaches. *J. of Coastal Research*, 17(2), 407-419.
- Stephens, S.A. (2012). Guidance on Assessing Extreme Sea Level in New Zealand, 12p. Tool 2.2.3 in NIWA, MWH, GNS and BRANZ (2012) *Impacts of Climate Change on Urban Infrastructure and the Built Environment: A Toolbox*.
- Stockdon, H.F., R.A. Holman, P.A. Howd, and A.H. Sallenger (2006). Empirical parameterization of setup, swash, and runup. *Coastal Engineering*, 53(7), 573-588.
- Storlazzi, C.D., Shope, J.B., Erikson, L.H., Hegermiller, C.A., and Barnard, P.L. (2015). Future wave and wind projections for United States and United States-affiliated Pacific Islands. U.S. Geological Survey Open-File Report 2015–1001, 426 p. <http://dx.doi.org/10.3133/ofr20151001>.
- Sweet, W. V., J. Park, J. J. Marra, C. Zervas, and S. Gill (2014). Sea level rise and nuisance flood frequency changes around the United States. NOAA Tech. Rep. NOS CO-OPS 73, 53 pp.
- Sweet, W.V. and J. Park (2014). From the extreme and the mean: Acceleration and tipping point of coastal inundation from sea level rise. *Earth Futures*, 2, 579-600. DOI: 10.1002/2014EF000272
- Sweet, W. V. and J. J. Marra (2014). 2014 State of Nuisance Tidal Flooding. A Supplement to the August 2015 U.S. State of the Climate Report. <http://www.noaaneews.noaa.gov/stories2015/2014%20State%20of%20Nuisance%20Tidal%20Flooding.pdf>

- Sweet, W. V. and J. J. Marra (2015). 2015 State of U.S. “Nuisance” Tidal Flooding. A Supplement to the August 2015 U.S. State of the Climate Report. <https://www.ncdc.noaa.gov/monitoring-content/sotc/national/2016/may/sweet-marra-nuisance-flooding-2015.pdf>
- Sweet, W.V., J. Park, S. Gill, and J. Marra (2015). New Ways to Measure Waves and Their Effects at NOAA Tide Gauges: A Hawaiian-Network Perspective. *Geophysical Research Letters*, 42, 9355–9361. doi:10.1002/2015GL066030.
- Sweet, W.V., R.E. Kopp, C.P. Weaver, J. Obeysekera, R.M. Horton, E.R. Thieler, and C. Zervas (2017). Global and Regional Sea Level Rise Scenarios for the United States. NOAA Tech. Rep. NOS CO-OPS 083, 75 pp.
- Tebaldi, C., Strauss, B.H. and Zervas, C.E. (2012). Modeling Sea Level Rise Impacts on Storm Surges Along U.S. Coasts. *Environmental Research Letters*, 7, 014032. DOI:10.1088/1748-9326/7/1/014032.
- Thompson, K.R., Bernier, N.B. and Chan, P. (2009). Extreme Sea Levels, Coastal Flooding and Climate Change with a Focus on Atlantic Canada. *Natural Hazards*, 51,139–150.
- Vitousek S., C.H. Fletcher, M.M. Barbee (2008). A practical approach to mapping extreme wave inundation: consequences of sea-level rise and coastal erosion. *Proceedings: Solution to Coastal Disaster 2008, Oahu, Hawaii, April 13-16*, p. 85-96.
- Vitousek, S., M.M. Barbee, C.H. Fletcher, B.M. Richmond, and A.S. Genz (2010). Pu‘ukoholā Heiau National Historic Site and Kaloko-Honokōhau Historical Park, Big Island of Hawai‘i: Coastal hazard analysis report. Natural Resource Technical Report NPS/NRPC/NRTR/GRD-2010/387. National Park Service, Fort Collins, Colorado.
- Zervas, C., (2005). Response of extreme storm tide levels to long-term sea-level change. *Proc. MTS/IEEE OCEANS 2005* (Washington, DC, 18–23 September) vol 3:2501–6.
- Zervas, C. (2013). *Extreme Water Levels of the United States 1893–2010*. NOAA Technical Report NOS CO-OPS 67. Silver Spring, Maryland: U.S. Department of Commerce, NOAA, National Ocean Service, Center for Operational Oceanographic Products and Services.

## Appendix: Additional Information pertaining to the TNC EESLR Web Tool

Information on flood frequency in the TNC EESLR Web Tool represents a blending of the two types of analyses described in the report “ Scenario-based Analysis of the Potential Impacts of Sea Level Rise on Coastal Flooding and Shoreline Retreat along the Kohala and Kona Coasts, from Kawaihae to Kailua-Kona, on the Island of Hawai‘i: METHODS AND RESULTS”. That is, it combines the analyses of flood frequencies derived from a normal distribution and flood extremes derived from a GEV distribution of observed water levels in tide gauges that were combined with probabilistic projections of future regional sea levels to determine the plausible range in changes in the SWL at different time periods. Further, it selects a preferred value from among the range of results of the analyses of flood frequencies, by establishing a frequency classification, and even then selecting a value from within this class. This is illustrated in the Table A-1, where the colors purple, blue, and yellow represent a range of days of flood frequency per year. In cases where there is a spread of frequencies across a range of elevations for a given scenario only one is selected for mapping purposes. For example, for 2050 where the elevation range for the “about once a week” class ranges from 1.0 to 1.1m (above MSL) the value shown on the map is 1.1m. Similarly, only one among the possible range of extremes (shown in red in Table A-1) is used for mapping purposes. Thus the map layers shown in the tool should be viewed as a simplification developed for demonstration purposes. They help to illustrate how information of this nature can be used to support resource management, community planning, for example. Parties seeking to use the map layers in the TNC tool for decision-making or other such purposes are advised to consult the Methods and Results Report so as to get a better understanding of the full breadth of the analysis and can better assess its potential implications.

Ht above MSL (m)		0.4	0.5	0.6	0.7	0.8	0.9	1	1.1	1.2	1.3	1.4	1.5	1.6	1.7	1.8	1.9	2	2.1	2.2	2.4	2.6	2.8	3	Extremes (m)
2030	LOW	347	288	188	85	22	2	0	0	0	0	0	0	0	0	0	0	0	0	0	0	0	0	0	0.9
	HIGH	364	353	303	210	103	30	4	0	0	0	0	0	0	0	0	0	0	0	0	0	0	0	0	1.2
2040	LOW	361	334	261	154	61	12	1	0	0	0	0	0	0	0	0	0	0	0	0	0	0	0	0	0.9
	MEDIUM	365	360	329	252	143	54	10	0	0	0	0	0	0	0	0	0	0	0	0	0	0	0	0	1.2
	HIGH	365	365	361	334	261	154	61	12	1	0	0	0	0	0	0	0	0	0	0	0	0	0	0	1.3
2050	LOW	364	357	317	232	123	41	6	0	0	0	0	0	0	0	0	0	0	0	0	0	0	0	0	1
	MEDIUM	365	365	363	343	279	176	77	18	1	0	0	0	0	0	0	0	0	0	0	0	0	0	0	1.3
	HIGH	365	365	365	365	360	329	252	143	54	10	0	0	0	0	0	0	0	0	0	0	0	0	0	1.5
2080	LOW	365	365	364	357	317	232	123	41	6	0	0	0	0	0	0	0	0	0	0	0	0	0	0	1.2
	MEDIUM	365	365	365	365	365	365	364	359	323	242	133	47	8	0	0	0	0	0	0	0	0	0	0	1.8
	HIGH	365	365	365	365	365	365	365	365	365	365	365	363	347	288	188	85	22	2	0	0	0	0	0	2.3
2100	LOW	365	365	365	365	361	334	261	154	61	12	1	0	0	0	0	0	0	0	0	0	0	0	0	1.4
	MEDIUM	365	365	365	365	365	365	365	365	365	365	364	357	317	232	123	41	6	0	0	0	0	0	0	2.2
	HIGH	365	365	365	365	365	365	365	365	365	365	365	365	365	365	365	365	365	365	361	261	61	1	0	2.9

- Elevations that experience flooding daily to every other day.
- Elevations that experience flooding once a week to once a month.
- Elevations that experience flooding once to several times a year.
- Elevations that flood in extreme SWL events (Once per decade).

**Table A-1. Flood frequency used in the TNC EESLR Web Tool.** The tool represents a blending of two analyses: flood frequencies derived from a normal distribution and flood extremes derived from a GEV distribution. Purple, blue, and yellow colors represent the range of days of flood frequency per year. Extremes highlighted in red are used for mapping purposes.